UNIVERSITY OF OSLO
Department of Geosciences
MetOs section

The hydrographic conditions in the upper Arctic Ocean from 1950 until 2009

Master thesis in Geosciences Meteorology and Oceanography

Inger-Lise Aasen

2nd June 2009

Acknowledgements

First and foremost, thank you Cecilie Mauritzen for all the supervision, for great ideas, and for never closing the door to your office. Thank you for including me in your projects and for the opportunities to go to Poland and Tromsø with the DAMOCLES and iAOOS projects. The trips were very inspiring! Also thank you Jan Erik Weber for supervision. Thanks to Kjell Andresen and Gunnar Wollan, always helping out when I felt like throwing the computer out of the window. Thanks to Pascaline Bourgain from the DAMOCLES-team for great help and many wonderful ideas, to Rasmus Benestad for help with FERRET, and to all the professors for being helpful whenever I've knocked at your doors. Thank you Øystein Godøy for helping out with the data organization, and for patiently trying to explain what meta data really is. Thank you Malin Rue for helping out with the downloading of the IPCC models. I acknowledge the modeling groups for making their model output available for analysis, the Program for Climate Model Diagnosis and Intercomparison (PCMDI) for collecting and archiving this data, and the WCRP's Working Group on Coupled Modelling (WGCM) for organizing the model data analysis activity. The WCRP CMIP3 multi-model dataset is supported by the Office of Science, U.S. Department of Energy.
I also wish to acknowledge the Ice-Tethered Profiler data, that were collected and made available by the Ice-Tethered Profiler Program based at the Woods Hole Oceanographic Institution
(http://www.whoi.edu/itp). Thanks to John Tool at the WHOI for helping out with the ITP data. Thanks too Igor Polyakov for making the NABOS data available to me, and to Wendy Ermold at the University of Washington for organizing the cruise data from Oden91, SCICEX93,-95,-96,-97,-98,-99,-2000, AOS94 and PolarStern93,-95 and -96.
I wish to acknowledge use of the Ferret program for analysis and graphics in the thesis. Ferret is a product of NOAA's Pacific Marine Environmental Laboratory. (Information is available at
http://ferret.pmel.noaa.gov/Ferret/).
To the girls at the study hall: You're great, and I'll miss you so much when school is over! Good luck with your thesis. And thank you so much, Kari Alterskjær, for reading through my thesis, for good comments and suggestions.

Abstract

I decided to take a fresh new look at the historical hydrographic data from the Environmental Working Group-atlas (EWG) in light of the recent dramatic changes, first and foremost to shed light on the cause of the large change in sea ice extent in the 21^{st} century.
Large changes in the hydrographic properties in the Arctic Ocean after the 1990s are evident, especially in depths and regions corresponding to Arctic Atlantic and Arctic Pacific waters. The changes started in the 1990s and continued in the beginning of the 21^{st} century.
The increase in Atlantic temperature in the inflow region is the most evident hydrographic change that has taken place. The Atlantic temperature in the region north of Spitsbergen is $3.5\pm0.8\,^{\circ}$C higher in the 21^{st} century compared to the historical data, whereas the changes are less in the Eurasian and Canadian Basins, with temperatures up to $0.5\pm0.4\,^{\circ}$C higher than the EWG climatology. The temperature increase is accompanied by salinification in the Atlantic Layer. The salinity north of Spitsbergen is 0.4 ± 0.2 units higher in the 21^{st} century compared to the historical data. The salinity in the other regions in the Arctic Ocean is higher with $0.2\text{-}0.3\pm0.1$ units. The density in the core of the Atlantic Layer has decreased due to the increased temperatures. The increased inflowing temperatures in the Atlantic Layer imply that the heat transported to the surrounding ocean must have increased in the 21^{st} century, since the rate of heating is less in the Eurasian and Canadian Basins. However there is a significant time lag between the regions, and this could partly explain the differences.
The Pacific Layer in the Canadian Basin is $0.1\text{-}0.6\pm0.425\,^{\circ}$C warmer in the 21^{st} century compared to the historical data. The Pacific temperature increase in the Canadian Basin is accompanied by a freshening in the 21^{st} century. The Pacific Water is up to 1 ± 0.125 unit fresher than in previous decades. The temperature increase and salinity decrease led to decreasing densities in the Pacific Layer.
There are events of warm pulses in the Atlantic Layer, and also in the Pacific Layer in the Canadian Basin. The anomalies propagate along the Arctic circulation. At depths corresponding to the Atlantic and Pacific layers there are positive anomalies in almost all years from the 1990s till present, and the anomalies are mainly larger in the 21^{st} century than in previous years. Thus the pulses in recent years are superimposed on a long term trend rather than being the main signal.
The observations imply that the sea ice cover in the Canadian Basin is closely linked to events of warm Pacific Water. The waters were especially warm in 2007, when a warm pulse that lasted for almost a year coincided with the sea ice extent minimum in 2007. In 2009 there is so far no such event of warm Pacific Water evident, and the outlook for the sea ice so far is not really hinting at an extreme year.
The interface between the cold Halocline Water and the underlying Atlantic Water has been lifted in the 21^{st} century, with up to 60 meters. The ascent started in the 1990s. Traditionally it has *not* been argued in favour of a close relationship between the sea ice and the Atlantic Layer because of the thick halocline layer, a cold vertically stable layer lying above the warm Atlantic Layer. However the observations show that this layer is thinning, meaning that the Atlantic influence on the sea ice will be more important in the future.

As an additional part of the thesis I have analysed model results from the **NCAR** and **HADLEY** models. The models are two of the global climate models used by the Intergovernmental Panel on Climate Changes (IPCC) in their assessment of the status of understanding the climate changes. Specifically, I have compared the NCAR and HADLEY models to observations, to see how well they simulate the changes seen in recent decades, both in ocean potential temperature and sea ice concentration.
The **NCAR** model reproduces the observed changes in ocean temperature and sea ice concentration in the Arctic fairly well. The negative trend in sea ice concentration is well reproduced, and the warming and lifting of the Atlantic Layer in recent decades are well simulated. However the Arctic circulation is not well represented in the model.
Also the **HADLEY** model reproduces the negative trend in sea ice concentration. However, there are no significant changes in ocean temperature from the 1950s till present, and the lifting of the Atlantic Layer going into the 21^{st} century is not reproduced by the model.
According to the models even larger changes are predicted in the 21^{st} century. The NCAR model predicts ice free summers by the end of this century. The loss of sea ice in both models is closely related to ascent and warming of the Atlantic water masses (though in the HADLEY model this process does not kick in until post the year 2000). Neither change occur in model runs without continued atmospheric forcing. I therefore argue that the ascent of the Atlantic Layer, which started in the 1990s is a key climate indicator which is important to continue monitor. Presently the warm Atlantic Water cannot affect the Arctic sea ice significantly because the warm water is covered by a thick layer of cold water (Halocline Water). As the analysis shows, this thick layer is thinning, and is projected to vanish within the 21^{st} century. The Arctic is a vulnerable region, and if this is a development which cannot be reversed we are facing large challenges in our immediate future.

Contents

1 Introduction

In the 21^{st} century large climate changes have been evident all over the world. Both the surface air temperatures and ocean temperatures have increased, and unusual patterns in precipitation and winds are observed, as well as sea-level rise, sea ice loss, changes in the freshwater supply and more extreme weather conditions. Glaciers all over the world have retreated. The effects of the global warming are a large challenge to economy, health and industrial development. The air temperature change during the 20^{th} century, both globally and regionally has been formally attributed to anthropogenic causes. The exploit on the planet earth will eventually have to stop.
The global warming is strongly modulated in the high northern latitudes of the Arctic Ocean. Simple monotonic trends do not exist, yet large changes are observed. The warming of the Arctic surface air temperatures have been almost twice as large as the global average in recent decades, which is known as the 'Arctic amplification' (Graversen et al., 2008). The heat capacity in the ocean is approximately 1000 times larger than in the atmosphere, and the net uptake of heat in the ocean since the 1960s are estimated to be approximately 20 times larger than in the atmosphere (Bindoff et al., 2007). The most visible change is the dramatic decrease in the sea ice cover in the 21^{st} century, and pictures of polar bears struggling for their lives have caught peoples attention and made scientists look north. September 2007 holds the record for a sea ice extent minimum, and even though the extent was larger in 2008, the total ice volume continued to decrease (NSIDC, 2008). In recent years there have been unusually much activity on the Arctic science field, both among glaciologists, oceanographers, biologists and meteorologists. The International Polar Year (IPY) from 2007-2008 is timed perfectly to monitor some of the largest changes we have observed in the Arctic so far.
I decided to take a fresh new look at the historic hydrographic data in light of the recent dramatic changes, first and foremost to shed light on the cause of the large change in sea ice extent in the 21^{st} century. I tried to answer the following questions:

- How much warmer has the Arctic Ocean become since the 1950s?
- What are the main hydrographic changes that have taken place?
- Are there some parts of the Arctic that has not really changed a lot?
- There is a lot of talk in the literature about warm pulses and propagation of these. Are these superimposed on a trend, or are they the main signal?
- How well do the IPCC models reproduce the changes seen at the end of the 20^{th} and in the beginning of the 21^{st} century, and what are Arctic's future prospect?
- Can these models shed any light on the significance of the changes we have seen in the Arctic hydrography?
- And last but not least: Is it possible that there are any connections between the observed changes in the ocean and the sea ice extent?

Chapter 2 gives the reader some background information on climate changes in the ocean, cryosphere and atmosphere observed at the end of the 20^{th} and in the beginning of the 21^{st} century, both global changes and changes in the Arctic, and also a brief introduction to the Arctic circulation system and geography. In chapter 3 the data, methods, uncertainties and software are presented. The results are presented in chapter 4. The general distribution of the water masses, hydrographic changes, changes in the depth of the interface between the Halocline Water and the underlying Atlantic Water, the extent and duration of warm pulses and model verification are presented. Possible connections between the Atlantic/Pacific waters and the sea ice are discussed in chapter 5, and also future predictions and the importance of continued anthropogenic forcing are discussed. The thesis ends with conclusions and final remarks in chapter 6.

2 Background

In chapter 2.1 the reader will get some general information about the climate changes observed in the ocean, cryosphere and atmosphere at the end of the 20^{th} and in the beginning of the 21^{st} century, both in a global and Arctic aspect. Chapter 2.2 gives a brief introduction on the Arctic Ocean's circulation system and geography.

2.1 Climate Change

2.1.1 The ocean

The Fourth Assessment Report of the Intergovernmental Panel on Climate Change (IPCC) (Bindoff et al., 2007) documents large changes in the global oceans in recent years, both in temperature, salinity, heat and in sea-level. From 1961-2003 there is observed a global averaged ocean temperature increase of approximately 0.10 °C in the upper 700 meters. Also large salinity trends are observed in the period 1955-1999. There are increased salinities in the Atlantic- and Indian water masses, the Pacific water masses are fresher than normal.
The global sea-level in recent decades rose with approximately $1.8 \pm 0.5 \frac{mm}{yr}$.
The sea-level is projected to rise further in the 21^{st} century (Meehl et al., 2007). The IPCC report presents different scenarios for future climate. The B1 model scenario is the most modest. The sea-level rise is here projected to be between 0.18-0.38 meters at the end of this century (2090-2099) compared to present (1980-1999), whereas the less modest A1F1 scenario projects changes between 0.26-0.59 meters. Approximately 50% of this sea level rise is due to thermal expansion, the rest of the contribution comes from run off and melting from glaciers, ice caps and the Greenland Ice sheet. The Antarctic Ice sheet is projected to contribute negative to the sea-level change, because increased snowfall and insignificant surface melting will lead to a gaining of mass. IPCC assessments suggest that deltas and small island states are particularly vulnerable to sea level rise.
Also the global ocean has a lower PH (Bindoff et al., 2007), the decrease has been approximately 0.02 units per decade. This is due to the increased uptake of carbon in the oceans. The ocean is now reaching the lowest PH value seen in 55 million years (Fosså, 2009). This can have large consequences, for example

the deep sea corals outside the Norwegian coast are in great danger of being extinct. The corals are the spawning ground and dining table to thousands of species, which are in great trouble without the deep sea corals.
In Arctic regions the hydrographic observations have been sparse due to the harsh climate and long polar nights. In recent years the activity has increased, and new methods for collecting data have been developed, for example the Ice Tethered Profilers used in this thesis, see chapter 3.1 for more details. Large changes are observed in the Arctic as well as in the global ocean. Polyakov et al. (2004) observed a rapid warming in the intermediate Atlantic Water of the Arctic Ocean over the 20^{th} century. They found that over recent decades, the data shows a warming and salinification of the Atlantic Layer accompanied by shoaling and probably thinning (more about the water masses in the upper Arctic Ocean in chapter 2.2). Also the estimated heat content in the Atlantic Layer averaged over the Arctic Ocean was larger by about $4.3 * 10^8 \frac{J}{m^2}$ in the 1990s compared to the 1970s (Rothrock et al., 1999). This component of Atlantic Water heat represents a flux of $0.4 - 0.6 \frac{W}{m^2}$. If reaching the surface, a flux of this size could cause 0.8-1.0 meters loss in ice thickness over the last 20 years or approximately the amount seen in recent decades.
Shimada et al. (2006) observed increased temperatures after the late 1990s in the Pacific Layer in the Arctic Ocean, accompanied by freshening.
Changes in the upper vertical structure in the 1990s are reported by Steele and Boyd (1998). During the SCICEX 1995 cruise the cold halocline, a stable layer lying above the warmer Atlantic Water, were absent in the Eurasian Basin, nevertheless it recovered in the late 1990s (Boyd et al., 2002). This was probably due to interruption of low salinity shelf water, changing the vertical salinity structure. The halocline protects the upper ocean from upward diffusion of heat from the Atlantic Layer. If the vertical structure is permanently weakened, the Atlantic influence will be larger at shallow depths. Boyd et al. (2002) estimated an increased heat flux of $1.26 \frac{W}{m^2}$ if the cold halocline layer is absent. A flux of this size could reduce the sea ice thickness with $0.15 \frac{m}{yr}$.

2.1.2 The cryosphere

The cryosphere, that is snow, river and lake ice, glaciers and ice caps, sea ice, frozen ground, ice shelves and ice sheets, has also undergone large changes in recent years.
The snow cover in the northern hemisphere has decreased from 1966-2005 in all months except November and December. The decreased snow cover is due to increased surface air temperatures, and the increased snow cover in November and December is due to increased precipitation. Also glaciers and ice caps have lost mass at a rate of $0.5 \pm 0.18 \frac{mm}{yr}$ (in sea-level equivalent) between 1961 and 2004. This negative trend is projected to continue and accelerate in the 21^{st} century, because summer melting dominates over winter precipitation (Meehl et al., 2007).
Changes in the permafrost are documented by the IPCC assessments, the temperature at the top of the permafrost layer has increased with up to 3 °C since the 1980s and the base has been thawing (Lemke et al., 2007). Going into the 21^{st} century the permafrost is projected to thaw further. Since a great amount of the efficient green house gas methane is bound in the permafrost, melting

will lead to a positive feedback process with increased amounts of methane in the atmosphere (Walsh, 2007).
The sea ice cover in the Arctic Ocean has also gone through large changes in recent decades. As mentioned in the introduction, September 2007 holds the record for the sea ice extent minimum (that is since the monitoring started in the 1970s), and the total sea ice volume continued to decrease in 2008 (NSIDC, 2008). There is a negative trend in the sea ice cover from the 1970s till present, as shown in figure 1(b) (September sea ice anomalies from Fetterer and Knowles (2008)). The ice extent was especially low in the area north of the Siberian and Alaskan coasts, that is in the Western Arctic Ocean, as shown in figure 1(a) (from NSIDC (2008)). There were also less ice than normal along the Atlantic side of the Arctic Ocean. Also the Northwest Passage, the shortcut between the Atlantic and Pacific Oceans, was almost completely clear, more open than ever monitored (that is since 1972), confirmed by analysts at the Canadian Ice Service and the U.S. National Ice Center (NSIDC, 2007). IPCC

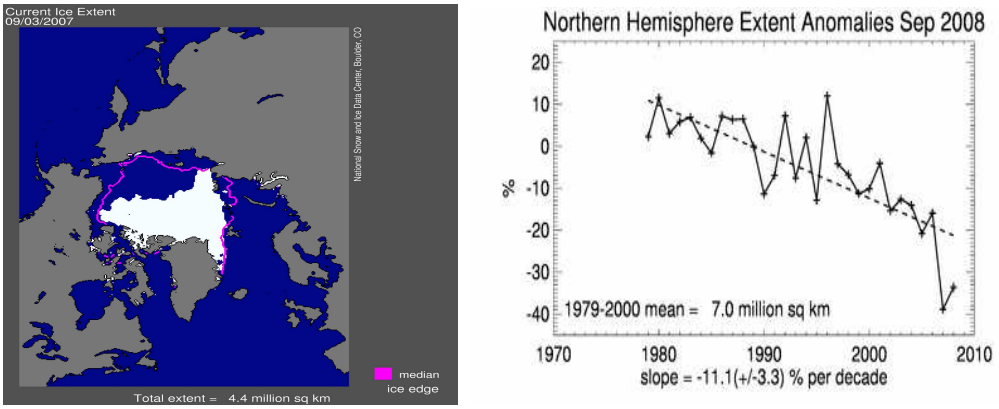

(a) (b)

Figure 1: (a): The ice extent in September 2007. The pink line is the median ice extent boarder. Figure from NSIDC (2008). (b): The sea ice anomalies for September months from 1979-2008 (the mean from 1979-2000 is used to estimate the anomalies). The slope is $-11.3 \pm 3.3\%$ per decade. Figure from Fetterer and Knowles (2008).

assessments suggest that since the surface air temperature north of 65 °N has increased with about twice the global average from 1965-2005, the decrease in ice mass is highly correlated with rising surface air temperatures (Lemke et al., 2007). The annual mean Arctic sea ice extent has decreased with $2.7 \pm 0.6\%$ per decade since 1975, and the decline is largest in the summer. The average sea ice thickness in the Central Arctic has decreased with up to 1 meter during the ten-years period from 1987-1997. Climate models calculate a strong reduction in the sea ice cover this century, and some of them calculate completely ice free summers (September) by the end of the 21^{st} century (with the high emission A2 scenario) (Walsh, 2007).
The decreased ice cover has major effects, because of many possible feedback

processes related to the sea ice melting. Since ice has a higher albedo than water, decreased ice cover means decreased albedo. This leads to a more efficient absorption of solar radiation, and the sea ice cover will decrease further. This is called the positive ice-albedo effect. Also the sea ice cover modifies the exchange of heat, gases and momentum between the atmosphere and the Arctic Ocean, without this 'lid' the ocean is much more exposed. The global thermohaline circulation can also be affected (Hassol, 2004). The thermohaline circulation refers to the large-scale ocean circulation driven by the global density gradients, created by the surface heat and freshwater fluxes. Sea ice formation rejects brine and makes the near surface waters saltier and denser. If the waters are dense enough they can sink and contribute to the formation of deep water and maintaining the global circulation. If the waters in the Arctic are made less salty because the temperature is not sufficiently cold to form sea ice, the formation rate of deep water will decrease, and the thermohaline circulation will be reduced. Weakened thermohaline circulation could lead to a negative feedback process because less heat from the tropical regions would be pulled northward by the ocean. Nevertheless there are many uncertain factors and also other possible feedback mechanisms associated with the loss of sea ice, so it is too early to tell what the extent of the consequences will be.

2.1.3 The atmosphere

IPCC assessments (Trenberth et al., 2007) report that the global surface temperature rose by $0.74 \pm 0.18\,^{\circ}\mathrm{C}$ over the last 100 years, see figure 2 from The Climatic Research Unit (CRU) (2008), and the rate of warming were almost twice as large the last 50 years compared to the rate for the last 100 years. 2005 was one of the two warmest years on the record. There are more frequently events of extreme weather since the 1970s, the number of heavy precipitation events is higher within many regions, and also droughts are more common, especially in the tropics and subtropics (Trenberth et al., 2007). Events of intense cyclone activity are also more common since the 1970s, and there is a change in the number of tropical storms and their tracks. Also changes in the large scale atmospheric circulation are apparent.

The surface air temperature in the Arctic has increased almost twice the global average, see figure 2 from Richter-Menge et al. (2008), and the temperature increase is consistent with the observed changes in the ocean and cryosphere (Lemke et al., 2007). The observed changes in the Arctic in the 1990s, both in the atmosphere, ocean and cryosphere, were often attributed to the large positive NAO/AO-index (North Atlantic Oscillation/Arctic Oscillation), that is the atmospheric pressure conditions. When positive NAO/AO-indexes are dominating there are increased pressure differences between the subtropical high and the Icelandic low, resulting in wind and water currents dragging relatively warm and salty Atlantic Water 20% further into the Arctic than usual (Visbeck, 2008). Polyakov et al. (2004) found that during positive NAO phases, there is warmer water from the North Atlantic into the Norwegian Sea, that is transported into the Arctic Ocean. However the changes in the Arctic have accelerated even though the NAO/AO-index has decreased in the 21^{st} century as shown in figure 3 (from the National Weather Service Climate Prediction Centre (2008)). This indicates that the NAO/AO-index alone can *not* explain the recent changes.

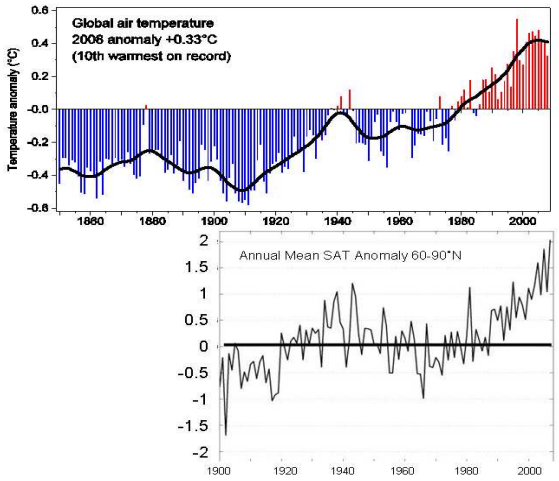

Figure 2: Upper figure: The combined global land and marine surface temperature anomaly record from 1850-2008 relative to the 1961-90 mean, from the HadCRUT3 data set from The Climatic Research Unit (CRU) (2008). Bottom figure: Arctic-wide surface air temperature anomaly record (60°-90°N) from 1900-2008 based on land stations north of 60°N relative to the 1961-90 mean, from the CRUTEM 3v data set from Richter-Menge et al. (2008). NOTE: Temperature scales not comparable.

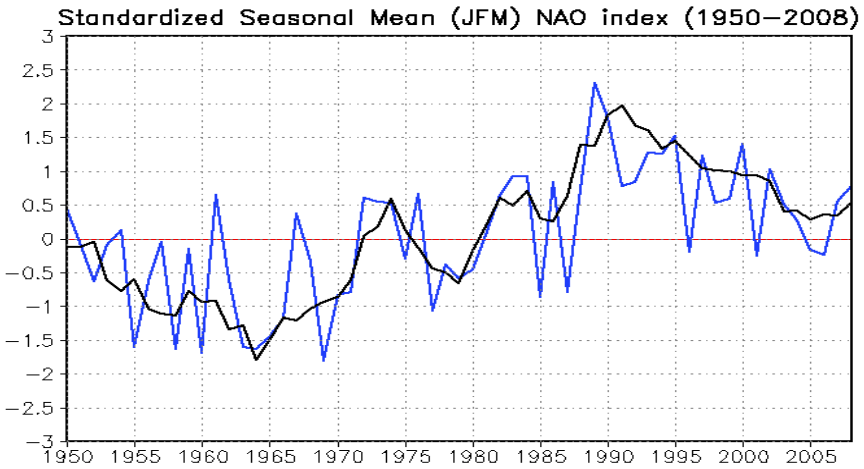

Figure 3: The blue line is the seasonal mean NAO during the cold season (January, February and March), and the black line is the standardized 5-years running mean of the index. The NAO-index has decreased after the mid-1990s, but the index is still positive. From National Weather Service Climate Prediction Centre (2008)

2.2 Arctic circulation system and geography

Figure 4 shows a bathymetric map over the Arctic Ocean (from National Geophysical Data Center (2001)). The Lomonosov Ridge, the Alpha-Mendelejev Ridge and the Laptev Sea is often referred to in the thesis. The Lomonosov Ridge is located from Ellesmere Island over the central part of the Arctic Ocean to the New Siberian Islands. The Alpha-Mendelejev Ridge is located towards the Canadian side of the Arctic Ocean. The Laptev Sea is located between the eastern coast of Siberia, Taimyr Peninsula, the Severnaya Zemlya and the New Siberian Islands, approximately 110-150 °E. The Eurasian Basin is located on the Eurasian side of the Lomonosov ridge, whereas the Canadian Basin is located on the Canadian side.

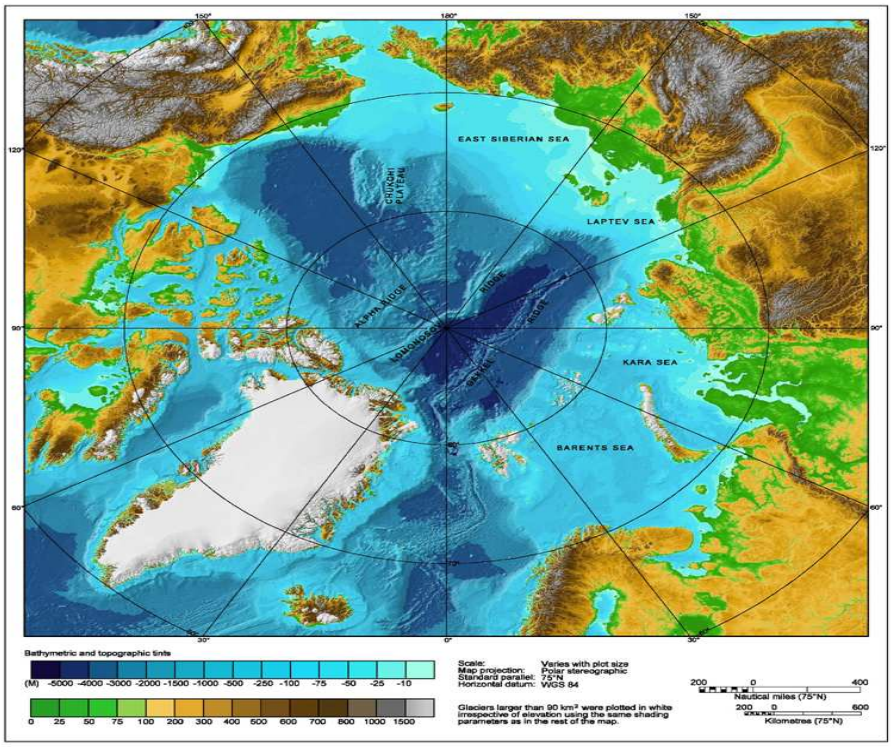

Figure 4: Bathymetric map over the Arctic Ocean from National Geophysical Data Center (2001)

A schematic of the circulation in the Arctic Ocean from Cook (2006) is shown in figure 6. The main entrance for Atlantic origin Water (relatively warm and salty water) into the Arctic Ocean is through the Fram Strait between Greenland and Spitsbergen, about 450 kilometers wide and 3000 meters deep. Another portion of the Atlantic Water comes from the Barents Sea branch of the North Atlantic Current. The Pacific origin Water (colder and fresher water) enters the Arctic Ocean through the shallow and narrow Bering Strait, 85 kilometers wide and 45 meters deep, between the Asian and North American continent (Knauss, 2005). There are also connections from the Arctic Ocean through the Canadian Archipelago by several channels, principally Nares Strait and Lancaster Sound.

These channels lead to Baffin Bay and thence to the Atlantic (Talley et al., 2009).

The Atlantic origin Water is found at approximately 200-800 meters depth. It is characterized by high temperatures (T>0 °C) and high salinities (S>34.8 units (Talley et al., 2009)). The Atlantic water masses run shallow, at approximately 100 meters, in the inflow regions, they cool and sink to larger depths as they enter the Arctic circulation system, following a cyclonic (anti-clockwise) circulation, see figure 6 (Cook, 2006). The Atlantic Water sinks to maximum depths in the Canadian Basin, with the core of Atlantic Water at approximately 350 meters. During that journey the Atlantic Water has cooled from approximately 3 °C close to the inflow region to approximately 0.5 °C in the Canadian Basin, see figure 5 from Coachman and Barnes (1963). The salinities are highest near the inflow region with salinities reaching 35.1 units, whereas the salinity in the Canadian Basin is down to approximately 34.7 units. The temperature decrease provides evidence that heat from the Atlantic Water is lost to the surroundings in the downstream propagation.

The Atlantic Water has been reported to be warmer and saltier at the end

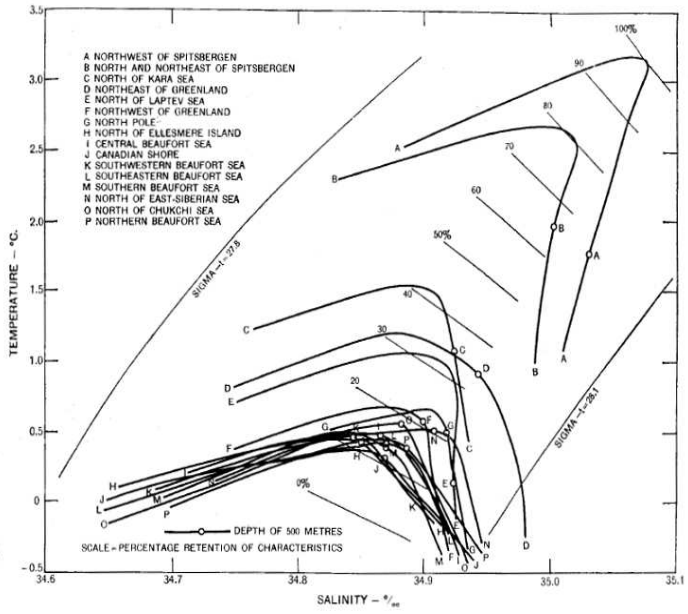

Figure 5: Temperature-salinity diagram for the Atlantic Layer in different location in the Arctic Ocean from Coachman and Barnes (1963). The temperatures and salinities are modified as the waters move away from the inflow region, whereas the densities remain fairly constant.

of the 20^{th} and in the beginning of the 21^{st} century, and a recent estimate by Schauer (2008) suggests that the heat content in the North Atlantic Current has

increased from 30 TW to 40 TW in the 21^{st} century. Since the heat content in the Atlantic Layer is high, upward diffusion of heat could significantly influence the sea ice cover. Nevertheless in most of the Arctic Ocean the Atlantic Water is protected from the surface by the cold halocline, a stable layer with a large vertical salinity gradient, which inhibit upward diffusion. The overlying Halocline Water is colder but less saline, making them less dense than the Atlantic Water.

The Pacific origin Water enters the Arctic Ocean and joins the Beaufort Gyre's anti-cyclonic (clockwise) circulation. Some of the Pacific Water joins the Transpolar drift and is transported out of the Arctic Ocean, see figure 6. The Pacific Water is characterized by low salinity (S<33 units) and temperature maximum warmer than -1 °C (Steele et al., 2004), low density and relatively high heat content compared to the surrounding water masses. The low density keeps the Pacific Water at shallow depths in the Arctic water column (Woodgate et al., 2008), and the Pacific Influence can be seen as a local temperature maximum at approximately 50-100 meters depth.
The Pacific Water is reported to be warmer and fresher at the end of the 20^{th} and in the beginning of the 21^{st} century. Shimada et al. (2001) found that the shallow temperature maximums carry enough heat within the upper layers to significantly affect the rate of ice cover and ice decay. Shimada et al. (2006) state that the area of low sea ice extent corresponds to the area where warm Pacific Summer Water is observed just beneath the surface mixed layer. They propose a positive feedback process as shown in figure 7 from Shimada et al. (2006). Less ice along the Alaskan coast in the winter months leads to a more efficient wind momentum transfer to the ice and underlying waters. This increases the sea ice motion and the upper ocean circulation, which in turn increases the oceanic heat transport into the western Canadian Basin (the Pacific Summer Water has the highest observed temperatures during winter). This retards the sea ice formation in winter, which accelerates the sea ice reduction. This means that even though the Pacific Water contains less heat than the Atlantic Water, it is likely to influence the sea ice cover due to its favorable position in the Arctic water column.

3 Data, methods and software

Chapter 3.1 starts out with an overview on the data used and also the geographic division of the data. The methods for defining the Atlantic and Pacific water masses are explained in chapter 3.2. The accuracies and seasonal variations are discussed in chapter 3.3. In chapter 3.4 an overview on the software used is given.

3.1 Data

3.1.1 1990-2008

Among several types of observational systems applied during IPY are Ice-Tethered ocean Profilers (ITP's). The Ice-Tethered Profile's data were collected

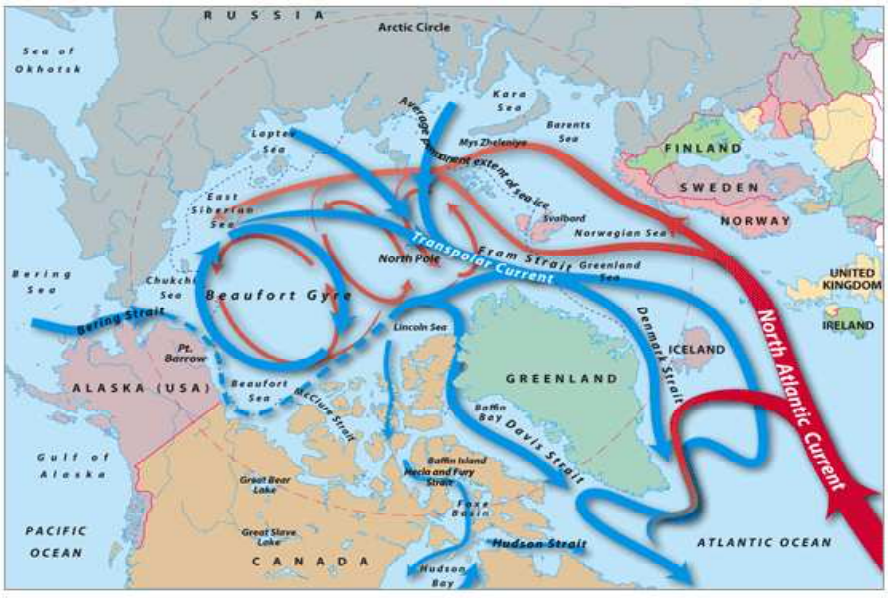

Figure 6: A schematic of the circulation in the Arctic Ocean, with the Atlantic (red) and Pacific (blue) water masses. Illustration from the Woods Hole Oceanographic Institution (Cook, 2006).

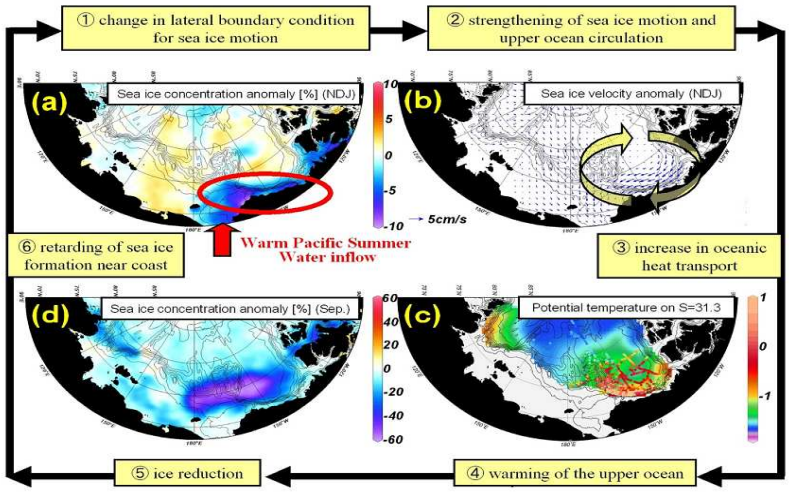

Figure 7: A feedback system in the Beaufort Gyre area from Shimada et al. (2006). Less ice along the Alaskan coast during winter leads to a strengthening of the sea ice motion and upper ocean circulation. This in turn leads to an increased oceanic heat transport and warming of the upper ocean. This reduces the ice formation during winter, and accelerate the sea ice reduction.

and made available by the Ice-Tethered Profiler Program based at the Woods Hole Oceanographic Institution (WHOI) (2007). The ITP's are moored into and drifting with the ice, mainly in the central Arctic Ocean and in the Beaufort Gyre, monitoring the upper 500-800 meters of the Arctic Ocean. They contain a CTD-profiler and provide us with profiles several times a day. They send the data onshore via satellites. I have used the data from 19 of these instruments (ITP1 till ITP19), from January 2004 till October 2008. I have used the so called level 2 real time data. Level 2 data are created from raw data (level 1) by automated routines at WHOI. The files are updated several times per day, and the data are averaged in 2-decibar (db) bins, but no response corrections, secondary calibration or editing are applied (Woods Hole Oceanographic Institution, 2007). Decibar (db) are units of pressure, where 1 pascal equals 0.0001 db. 1 db is approximately 1 meter at shallow depths, whereas the difference between them is larger at larger depths. I have also added data from the Nansen and Amundsen Basin Observational Systems (NABOS) cruises (August/September 2004-2007). The 21^{st} century data cover the area shown in figure 8(b). For the 1990s I analysed hydrographic data from the following expeditions: Oden91, SCICEX93,-95,-96,-97,-98,-99,-2000, AOS94 and PolarStern93,-95 and -96, provided by Wendy Ermold at the University of Washington. The data coverage for the 1990s is shown in figure 8(a).

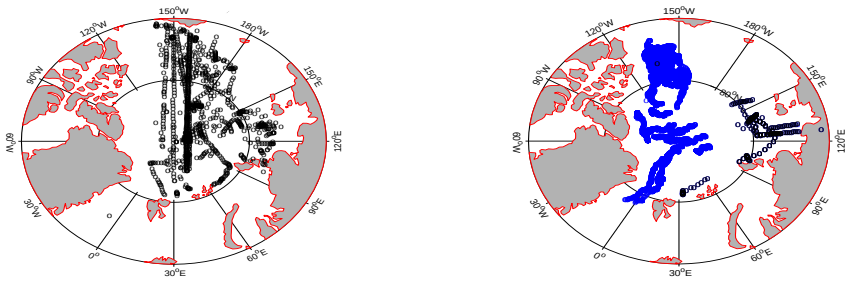

(a) (b)

Figure 8: (a): The observations from Oden, SCICEX, AOS and PolarStern cruises collected in the 1990s. (b): The observations from the ITP's (blue) and NABOS (black) cruises from January 2004 till October 2008.

3.1.2 Historical data: EWG data set

For comparison with the modern data I downloaded the Environmental Working Group-Atlas (Arctic Climatology Project, 2000). This atlas is a gridded collection of winter data (October-May) from 1950-1990, and covers all of the Arctic Ocean. Different interpolation methods are provided, I mainly used the data that was spectrally interpolated. The quality and accuracy of the data depends on the amount of data collected for the different years, and also the methods used for data sampling and interpolation. A detailed discussion of the accuracy is given in chapter 3.3.

3.1.3 Geographic division

The data coverage does not allow a full scale analyses of the temporal evolution of hydrography in the entire Arctic Ocean. To ease the comparison between the gridded EWG data set and the single CTD observations I split the Arctic Ocean into 9 smaller parts. The splitting of the Arctic is chosen so that the ITP and NABOS data covers as much of the areas as possible, and also so that some topography is followed. The nine smaller boxes cover the areas shown in figure 9 (a). Thereafter I grouped the 9 boxes into 4 major areas, which represent different hydrographic domains, as shown in figure 9 (b).

The region west of Spitsbergen (pink box) was omitted from the further dis-

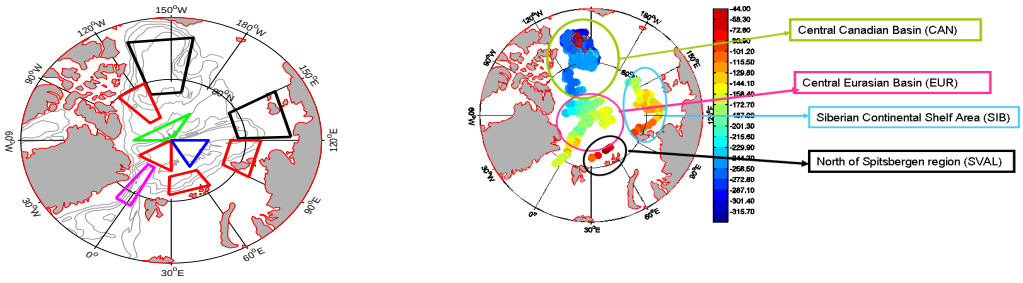

(a) (b)

Figure 9: (a): The division of the Arctic Ocean into 9 smaller boxes. There is one box north of Spitsbergen (red (81-84N,28-65E)) and two in the Laptev Sea (red (74-81N,122-150E) and black (78-82N,90-120E)) in the Siberian Continental Shelf Area. There are three parts around the north pole, two on the Eurasian side of the Lomonosov Ridge (red (85-90N,30W-30E) and blue (85-90N, 60-120E)) and one on the Canadian side (green (85-89N,60-180W)). Also there is one box west of Spitsbergen (pink (75-85N,8W-3E)), and two boxes in the Canadian Basin, one box in the Beaufort Gyre (black (l73-82N,130-160W)), and one box north of the Beaufort Gyre (red (80-86N,105-129W)). (b): The four hydrographic domains in the Arctic Ocean covered by the ITP and NABOS data: the North of Spitsbergen Region (SVAL), the Siberian Continental Shelf Area (SIB), the Central Eurasian Basin (EUR) and the Central Canadian Basin (CAN).

cussion, since the ITP-data in this region come from the outflowing ice at the end of the ITP's journey and the interpolation method in the EWG-atlas causes the outflow area to be influenced by the warmer West-Spitsbergen current.

The figures in the thesis are labeled with the abbreviations corresponding to the four main domains, 'SVAL' (North of Spitsbergen Region, one red box), 'SIB' (Siberian Continental Shelf Area, red and black box near the Laptev Sea), 'EUR' (Central Eurasian Basin, cover the red, blue and green box located along

the Lomonosov Ridge) and 'CAN' (Central Canadian Basin, red and black box near the Beaufort Gyre). The figures line colors coincide with the box colors.

3.2 Water mass definitions

As mentioned in chapter 2.2 there are two main water masses in the upper Arctic Ocean: The Atlantic and Pacific water masses. The Atlantic Water can be seen as a temperature maximum at approximately 200-800 meters, whereas the influence of Pacific Water is seen as a shallow temperature maximum at approximately 50-100 meters depth, see figure 10 and 11. Figure 10 shows a typical vertical cross section of the Arctic Ocean. The figure shows a potential temperature Hovmoller diagram for ITP2 during a 40 days drift. Since the ITP's monitor the upper 500-800 meters of the Arctic Ocean, hydrographic changes at larger depths are not investigated. ITP2 is drifting in the Beaufort Gyre, and was deployed in July 2004. The Pacific Water can be seen as higher temperatures at approximately 50-100 meters depth. The core of the Atlantic Water can be seen at approximately 300 meters depth. The temperature in the Atlantic Water decreases and the Atlantic Layer runs deeper as the ITP drifts further away from the inflow region.
Since I wanted to search for changes in the Pacific and Atlantic water masses I needed to find criteria to define them, so that I could map out their influence in the Arctic Ocean. This was done in collaboration with the French PhD-student Pascaline Bourgain from the DAMOCLES-team. Indexes for the strength of the influence of the two water masses were calculated: one **Pacific Water Influence-index** (PWI-index) and one **Atlantic Water Influence-index** (AWI-index), shown in chapters 3.2.1 and 3.2.2. A large PWI- or AWI-index implies that there is a large amount of heat within the layer which can influence the surrounding waters. The vertical resolution in the EWG atlas was too poor for these definitions, so the methods were only tested on the data from 1990-2008. I tried to collect data with good vertical resolution from before 1990, with great help from Wendy Ermold at the University of Washington, but the data was too geographically limited and could therefore not be used for comparison with the other data. For defining the different water masses I extrapolated all the data into 1 db bins. To avoid noise the temperature- and salinity gradients were interpolated in 5 db bins, and a moving average was estimated to smooth the profiles. Figure 11 shows the methods described below on a random temperature profile.

3.2.1 Atlantic Water Influence-index (AWI-index)

The Atlantic Water Influence-index **(AWI-index)** is calculated as the temperature difference between the Atlantic temperature maximum and the temperature at the start of the thermocline, see figure 11. The Atlantic temperature maximum is defined as the maximum temperature between 200-550 db.
The thermocline is the area with the largest vertical temperature gradient, and starts out at depths between 20 and 200 db. The depth of the start of the thermocline is defined as the depth where the temperature gradient shifts from approximately zero too larger than zero (gradT>0.001 °C). Below this point the temperature must continue to increase in a depth range of at least 60 db. If

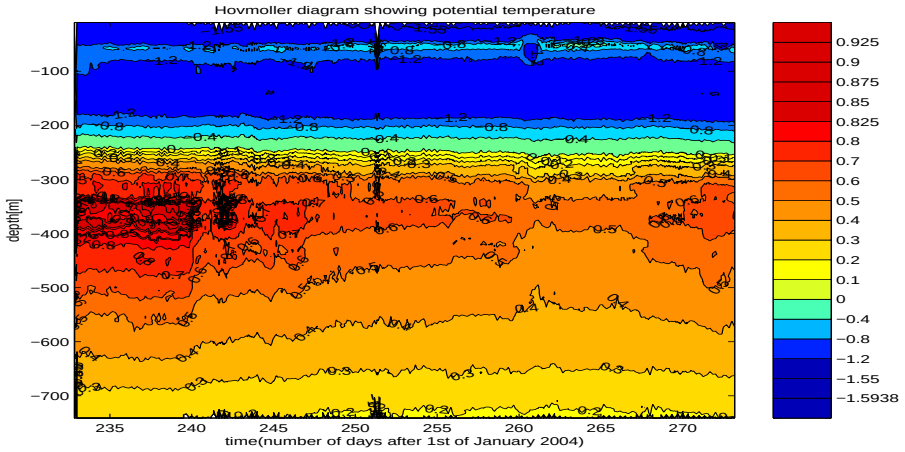

Figure 10: Potential temperature during a 40 days period for ITP 2, deployed in July 2004. ITP2 drifts in the Beaufort Gyre. Pacific Water is evident at approximately 50-100 meters. The warm core of Atlantic Water starts at approximately 300 meters.

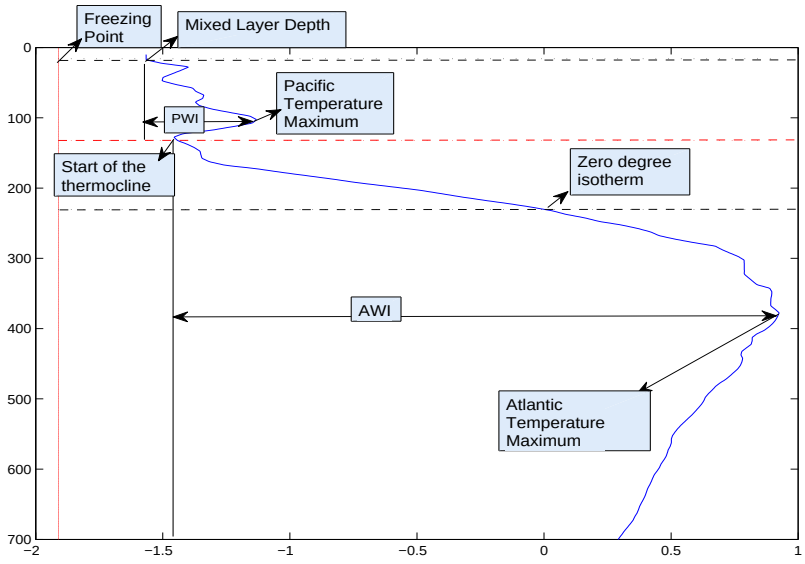

Figure 11: The methods used for defining the different water masses used on a random temperature profile (itp profile number 100): Vertical red line indicates the freezing point. The upper black dotted line is the end of the mixed layer (mixed layer depth). The red dotted line is the start of the thermocline. The lower black dotted line is the zero degree isotherm. The Pacific Water Influence-index is defined as the temperature difference between the shallow Pacific temperature maximum and the temperature in the mixed layer depth. The Atlantic Water Influence-index is defined as the temperature difference between the Atlantic temperature maximum and the temperature at the start of the thermocline.

no points fulfill these criteria they are relaxed, the depth range where the temperature has to increase is reduced to 40 db, but the gradient has to be larger, that is gradT>0.006 °C. Some profiles have more than one point fulfilling these criteria, and if the points are in the same temperature range (the ratio between them is between 0.5 and 1.5), the deepest one of them is chosen as the point where the thermocline starts. If the points have significantly different temperature, one of them lies below the start of the thermocline, and the upper one of them is chosen as the start of the thermocline. If no points fulfill these criteria, there is no Atlantic influence in the specific profile meaning that the AWI-index is 0.

3.2.2 Pacific Water Influence-index (PWI-index)

The influence of Pacific Water is seen as a shallow temperature maximum at approximately 50-100 meters depth, see figure 11. The Pacific temperature maximum is therefore defined as the maximum temperature between the mixed layer depth and 150 meters. The Pacific Water Influence-index (**PWI-index**) is estimated as the difference between the Pacific temperature maximum and the temperature in the mixed layer depth.
The mixed layer depth is located somewhere between the surface and the start of the thermocline. The criteria for finding the mixed layer depths is that the vertical temperature gradients and salinity gradients have to be small, close to zero (gradT$\leq$0.005 °C and gradS$\leq$0.005 units). Also the temperature difference between the shallowest observation and the observation at the end of the mixed layer has to be less than 0.01 °C, the salinity difference less than 0.1 units. If the temperature criterion and salinity criterion are not fulfilled at the same depths, the most shallow of them is chosen as the mixed layer depth. If no mixed layer depth is found 36 meters is chosen as the mixed layer depth (after investigation of different profiles).
To make sure that the temperature maximum found is the real Pacific maximum we need to check that this is a local temperature maximum, meaning that the gradient shifts from positive to negative above the thermocline. Also the salinity in the temperature maximum has to be less than 33 units, and the temperature in the mixed layer depth has to be less than 0 °C. If these criteria are not fulfilled, there is no Pacific influence in the specific profile, meaning that the PWI-index is 0.

3.3 Uncertainties

3.3.1 Under sampling, spatial and temporal averaging of the data

When comparing the historical EWG atlas with modern CTD data, uncertainties are introduced into the results. The uncertainties mainly come from under sampling and also spatial and temporal averaging of the data. Grotenfendt et al. (2008) applied an uncertainty of 0.7 K in the inflow region and 0.4 K in the interior basins for the EWG data in their comparison with the modern data. This appears to be a very conservative estimate, but since this is the only estimate mentioned in literature I will nevertheless use it. Unfortunately Grotenfendt does not provide an error estimate for the salinity. A rule of thumb is that the errors in salinity are 1/10 of the errors in temperature. A 'conservative

guess' for the estimated uncertainty in salinity is 0.1 units, this is the estimate I will use. I will use the same error estimates for the modern ITP and cruise data (although the errors assumed to cover the ITP instrumental accuracy are estimated as $\pm 0.001\,^{\circ}C$ (Timmermans et al., 2008), but my estimates include errors introduced by under sampling as well).

3.3.2 Seasonal Variations

Since the historical EWG data set is a collection of winter data (October-May) whereas the ITP's have data covering all months and NABOS have data for August/September I needed to quantify the errors imposed by using data from different seasons, mainly in the Atlantic and Pacific layers. Figure 12 shows the mean potential temperature and salinity profiles for all data sampled by the ITP's in the Beaufort Gyre in the Canadian Basin .
The difference when comparing all year data with winter data is not large in the Eurasian and Canadian Basins. In the **Eurasian Basin** the upper 50 meters are $0.025\,^{\circ}C$ warmer when using all year data, but below that there are no significant differences. The Eurasian Basin salinity is 0.25 units fresher in the upper 30 meters due to seasonal variations. Below 30 meters there are insignificant seasonal differences in salinity.
The **Canadian Basin** exhibits a seasonal variability in temperature of approximately $0.1\,^{\circ}C$ in the upper 30 meters, while depths corresponding to the Pacific temperature maximum have temperature variability up to $0.025\,^{\circ}C$. At larger depths there is no significant seasonal variability in temperature. The salinity variability is up to 0.025 units in the upper 70 meters, at larger depths the salinity has insignificant seasonal variability.
North of Spitsbergen and the **Siberian Continental Shelf Area** are covered by summer data only. From the Eurasian and Canadian Basins the largest variability in temperature when comparing summer data with winter data is up to $0.2\,^{\circ}C$ in the upper 30 meters (warmer summer data), the Pacific temperature maximum has $0.15\,^{\circ}C$ warmer temperatures during summer. At larger depths the temperatures are up to $0.1\,^{\circ}C$ warmer during summer. The variability in salinity when comparing summer data with winter data is up to 1.5 units (fresher summer data) in the upper 70 meters, below that the winter waters are saltier with up to 0.1 units.
This means that in the Atlantic Layer I can compare winter data from the EWG-atlas with all year data in the Eurasian and Canadian Basins, without introducing larger uncertainties into the analyses. North of Spitsbergen and in the Siberian Continental Shelf Area I will use $0.1\,^{\circ}C$ and 0.1 units as the errors in temperature and salinity in the Atlantic Layer due to seasonal variability. In the Pacific Layer I will add an uncertainty of $0.025\,^{\circ}C$ in temperature and 0.025 units in salinity due to seasonal variability.
The error in the depth of the upper interface between Halocline Water and the underlying Atlantic Water by comparing summer data with winter data is approximately 10 meters. When comparing summer data with all year data the error is less than 3 meters in the Canadian Basin and 8 meters in the Eurasian Basin. Therefore I will use 10 meters as the error in the depth of the upper interface between the cold Halocline Water and Atlantic Water.

The uncertainties are summarized in figure 13, they are the sum of the uncer-

tainties related to under sampling and also spatial and temporal averaging of the data, and the uncertainties related to the different data sampling seasons.

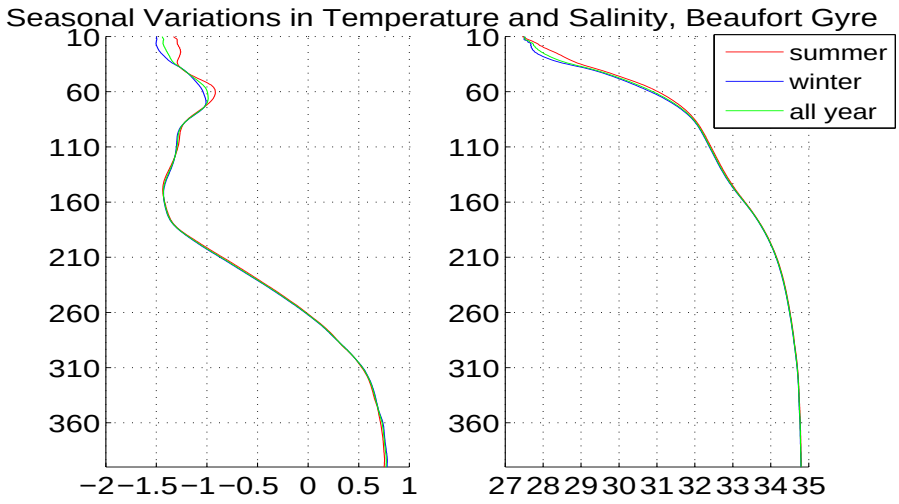

Figure 12: The potential temperature (left) and salinity (right) in the Beaufort Gyre in the Canadian Basin, summer data (red), winter data (blue) and all-year averaged data (green). Depths corresponding to the Pacific temperature maximum (approximately 60 meters depth) have variability up to 0.025 °C and 0.025 psu units. Insignificant seasonal variability in the Atlantic Layer.

3.4 Software

Most of the scripts and figures in the thesis are made in MATLAB. From the web, I downloaded two additional tools for MATLAB, one mapping-tool, **m-map**, made available by Rich Pawlowicz (Pawlowicz, 2005), and a seawater toolkit, **seawater**, by Phil Morgan (Morgan and Pender, 2006). The first one makes it easy to give a geographical presentation of the data, and the latter is a handy tool for conversion of different seawater properties. The potential temperature conversions are made with the seawater tool (Morgan and Pender, 2006), and follow UNESCO 1983 conventions. The potential density calculations are also made with UNESCO's 1983 polynomial. The plotting tool FERRET was used in the analyses of the NCAR and HADLEY models.

4 Results

Chapter 4.1 explains the general distribution of the water masses in the upper Arctic Ocean in the 1990s and in the beginning of the 21^{st} century. The hydrographic changes in the Atlantic and Pacific layers from 1950 till 2008 are presented in chapter 4.2, followed by changes in the depth of the upper interface between the cold halocline waters and Atlantic waters in chapter 4.3. The duration and spreading of warm pulses are investigated in chapter 4.4.

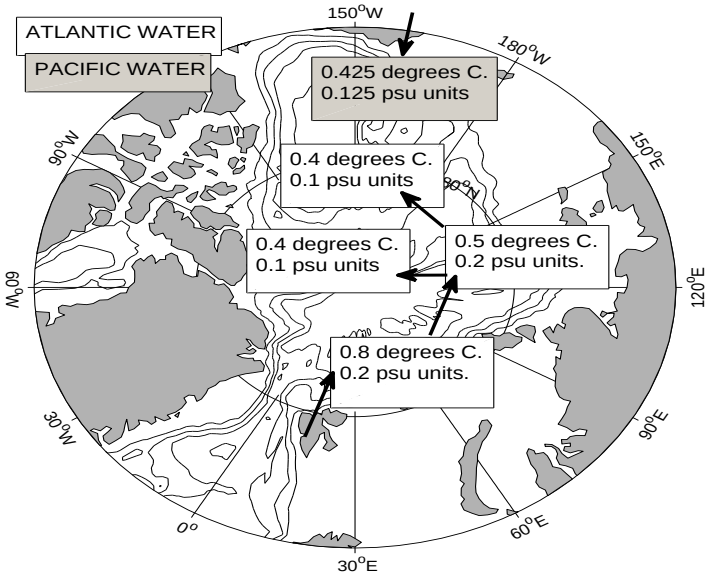

Figure 13: The uncertainties from under sampling, seasonal variations and spatial and temporal averaging of the data for the Atlantic (white) and Pacific waters (gray).

Chapter 4.5 presents how well the NCAR and HADLEY models simulate the hydrographic changes observed in recent decades.

4.1 General distribution of the water masses in the upper Arctic Ocean

There are two main water masses in the upper Arctic Ocean, namely **Atlantic Water**, found at approximately 200-800 meters depth lying below the cold halocline waters, and **Pacific Water** found in the upper 100 meters. To map out their influence in the 1990s and in the beginning of the 21^{st} century an **Atlantic Water Influence**-index (AWI-index) and a **Pacific Water Influence**-index (PWI-index) were defined in chapter 3.2. The indexes are given in °C, and they are the temperature differences between the Atlantic/Pacific temperature maximums and the surrounding temperatures. A large PWI- or AWI-index implies that there is a large amount of heat within the layer which can influence the surrounding waters.
Figure 14 shows the distribution and influence of the Atlantic and Pacific waters in the 1990s and from 2004 till 2008. Black color indicates no Pacific/Atlantic influence, meaning that the PWI-index is less than 0.1 °C, AWI-index less than 0.05 °C.
The Atlantic influence can be seen in the entire Arctic Ocean, with the highest temperatures close to the Fram Strait on the Eurasian side of the Lomonosov Ridge, and the lowest temperatures in the Canadian Basin, as we would expect from the general circulation discussed in chapter 2.2. Generally Pacific Water is found on the Canadian side of the Lomonosov Ridge, with the highest tem-

peratures close to the Bering Strait.
As the Atlantic and Pacific waters circulate into the Arctic Ocean, heat is lost to the surrounding ocean, the hydrographic properties are modified by the cold Arctic surroundings, and the PWI- and AWI-indexes decrease. As the Atlantic Water cools it deepens, the upper interface between the Halocline Water and Atlantic Water deepens from approximately 100 meters near the Fram Strait, to 180 meters in the Laptev Sea, deeper than 200 meters on the Eurasian side of the Lomonosov Ridge, and sinks to 300 meters in the Beaufort Gyre area.
A possible 'front', that is a boarder line between the Atlantic and Pacific regimes, are drawn as a red line in figure 14(b) and (d), and the result suggests that the boarder line in the 21^{st} century lies on the Canadian side of the Lomonosov Ridge. Literature suggests the this boarder line has shifted from the Lomonosov Ridge to the Alpha-Mendelejev Ridge (Nishino et al., 2008), which is in good accordance with my results. Boyd et al. (2002) found an eastward shift in the boundary between Atlantic and Pacific origin waters, such that the Atlantic Water covered 20% more of the central Arctic than previously. The results confirm that all of the 9 boxes the Arctic Ocean was divided into (figure 9(a)) exhibit Atlantic Influence. There is no Pacific influence (PWI-index<0.1 °C) in the Laptev Sea, in the region north of Spitsbergen or in the west of Spitsbergen region, neither in the two boxes on the Eurasian Side of the Lomonosov Ridge. This means that three of the nine small boxes have Pacific Influence, namely the green box on the Canadian side of the Lomonosov Ridge, and the red and black box in the Beaufort Gyre area in the Canadian Basin. The classifications of the two main water masses are helpful in the further analyses.

4.2 Hydrographic changes in the Arctic Ocean from 1950 till 2008

Large changes in temperature and salinity are reported at the end of the 20^{th} and in the beginning of the 21^{st} century, both in Atlantic (warming and salinification) and Pacific (warming and freshening) waters. I have compared modern CTD data from 1990 till 2008 with the historical EWG atlas (1950 till 1990) to map out changes in potential temperature, salinity and potential density. Changes were investigated in 5m, 10m, 25m, 50m, 75m, 100m, 150m, 200m, 250m, 300m, 400m and 500m depth, since these are the depths given in the EWG data set that correspond with the modern data. The hydrographic data from the EWG atlas are ten years averaged, so the data from the 1990s were averaged, and also the ITP- and NABOS data from 2004-2008 to represent the beginning of the 21^{st} century (that is 5 years average). The temperature and density anomalies were calculated with the averaged 1950 till 1990 data as the reference value, so that positive anomalies indicate higher temperatures/densities than the historical data.
I have found large changes in temperature, salinity and density, especially at depths and in regions corresponding to Atlantic and Pacific water masses (chapter 4.2.1 and 4.2.2 respectively) after the 1990s. The largest changes in the Atlantic Layer (warming and salinification) are found in the inflow region north of Spitsbergen, with smaller changes in the Eurasian and Canadian Basins, whereas the largest changes in the Pacific Water (warming and freshen-

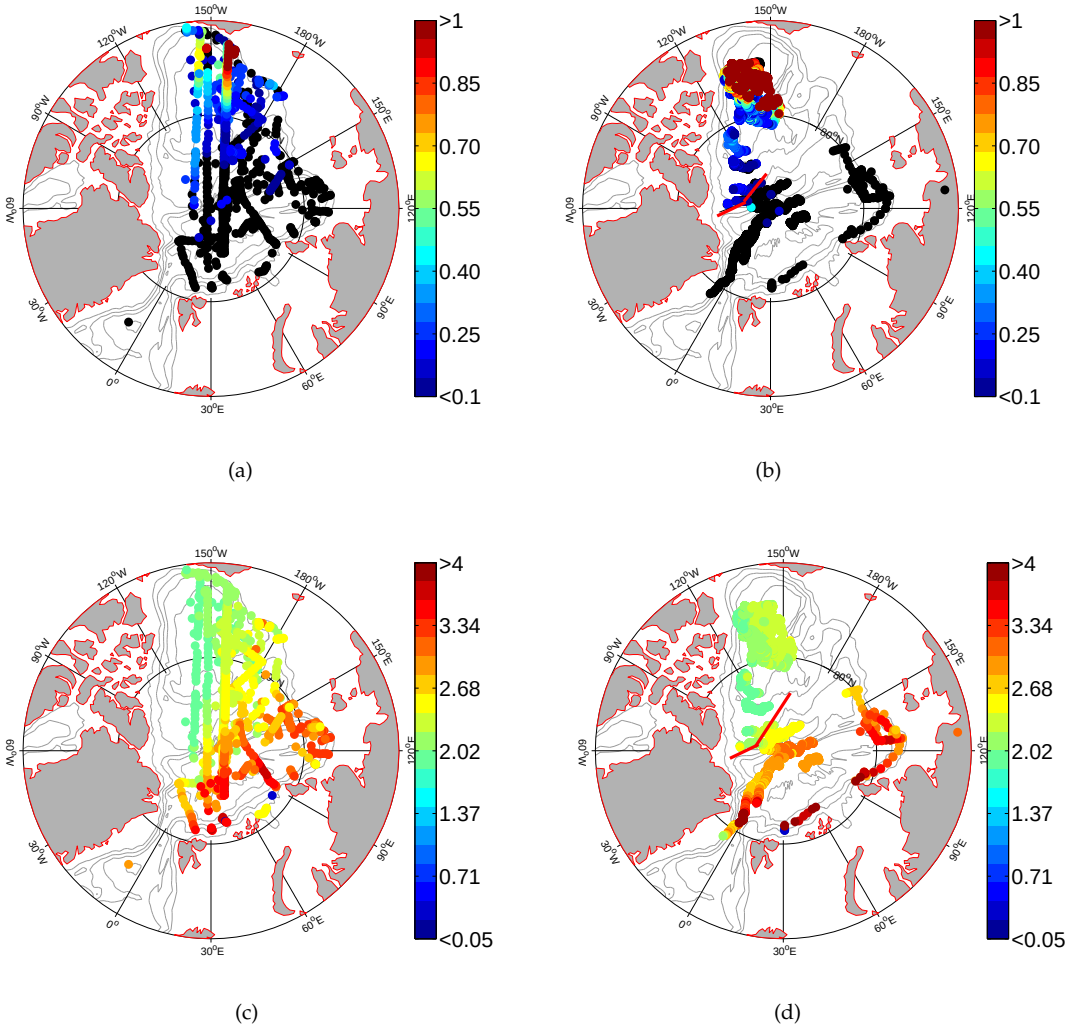

Figure 14: Maps showing the Pacific Water Influence-index (PWI-index) ((a) the 1990s and (b) 2004-2008), and the Atlantic Water Influence-index (AWI-index) ((c) 1990s and (d) 2004-2008). The largest AWI-indexes are seen near the Fram Strait, and the largest PWI-indexes are found close to the Bering Strait, as we would expect from the general circulation patterns. A possible front between the Atlantic and Pacific waters in the 21^{st} century is drawn in red. Black color indicates no influence.

ing) are found in the Beaufort Gyre in the Canadian Basin. Figure 15 shows time series from 1950-2008 of the potential temperature, salinity and potential density for the north of Spitsbergen region (SVAL), the Laptev Sea in the Siberian Continental Shelf Area (SIB), the Central Eurasian Basin (EUR) (where the Eurasian Basin consists of the red and blue boxes on the Eurasian side of the Lomonosov Ridge) and in the Beaufort Gyre in the Canadian Basin (CAN). Note that the vertical resolution in the historical data (1950-1990) is coarse (5db, 25db, 50db and 100 db depending on the depth), whereas the resolution after 1990 is 5 db.

Figure 15 shows that the Atlantic Water is warmer and saltier at the end of the 20^{th} and in the beginning of the 21^{st} century compared to the historical data. The core of the Atlantic Water is less dense than the historical data (pre-1990s) due to the large temperature increase despite the increased salinity. Nevertheless the waters are denser than the historical data from the top of the Atlantic Layer and down to the core, due to increased salinities. The Pacific Water can be seen in the Canadian Basin. The waters are warmer and fresher at the end of the 20^{th} and in the beginning of the 21^{st} century compared to the historical data. This makes the Pacific Water less dense in recent years.

4.2.1 Changes in the Atlantic Water

The temperature increase in the Atlantic Layer is largest in the region **north of Spitsbergen**. The Atlantic Layer temperatures are up to $3.5\pm0.8\,^{\circ}$C higher than the pre-1990s data, see figure 16 for the temperatures, salinities and density anomalies in the core of the Atlantic Layer (at approximately 200 db depth). The largest increase in temperature occurs at depths shallower than 200 db, but the temperature increase is up to $1\pm0.8\,^{\circ}$C at larger depths as well. The temperature anomalies in the north of Spitsbergen region reach nearly $3\pm0.8\,^{\circ}$C in the 21^{st} century. The temperature increase after the 1980s is accompanied by a salinity increase of up to 0.4 ± 0.2 units in the 21^{st} century data. Nevertheless there is a peak in salinity in the 1970s with values comparable to the 1990s salinity. The density anomalies in the core of the Atlantic Layer are negative after the 1980s, meaning that the waters are less dense than the historical EWG data due to the increased temperatures. All of the changes seen in this region are increasing from the 1990s into the 21^{st} century, with higher averaged temperatures and salinities monitored in the 21^{st} century, just as found by Polyakov et al. (2004) and Cokelet et al. (2008).

When following the circulation of the Atlantic Water into the Arctic Ocean the current flows along the **Siberian Continental Shelf Area** and into the Laptev Sea. The warming and salinification in the Atlantic Layer is large here as well, nevertheless not as large as in the inflow region. The increase in the Atlantic Water temperature after the 1980s is between $0.4\text{-}1.5\pm0.5\,^{\circ}$C, whereas the temperature anomalies are between $0.4\text{-}0.8\pm0.5\,^{\circ}$C. The salinities in the Atlantic Layer are up to 0.3 ± 0.2 units larger than the historical data. The variability in the Atlantic Layer is large with high temperatures in the 1950s, some depths have temperatures comparable to today's temperatures. However the temperatures in the 21^{st} century are significantly higher than the temperatures in the 1980s, see figure 17 for the temperatures, salinities and density anomalies in the core of the Atlantic Layer (at approximately 250 db depth) in the red and black box located near the Laptev Sea (SIB). The density anomalies are small

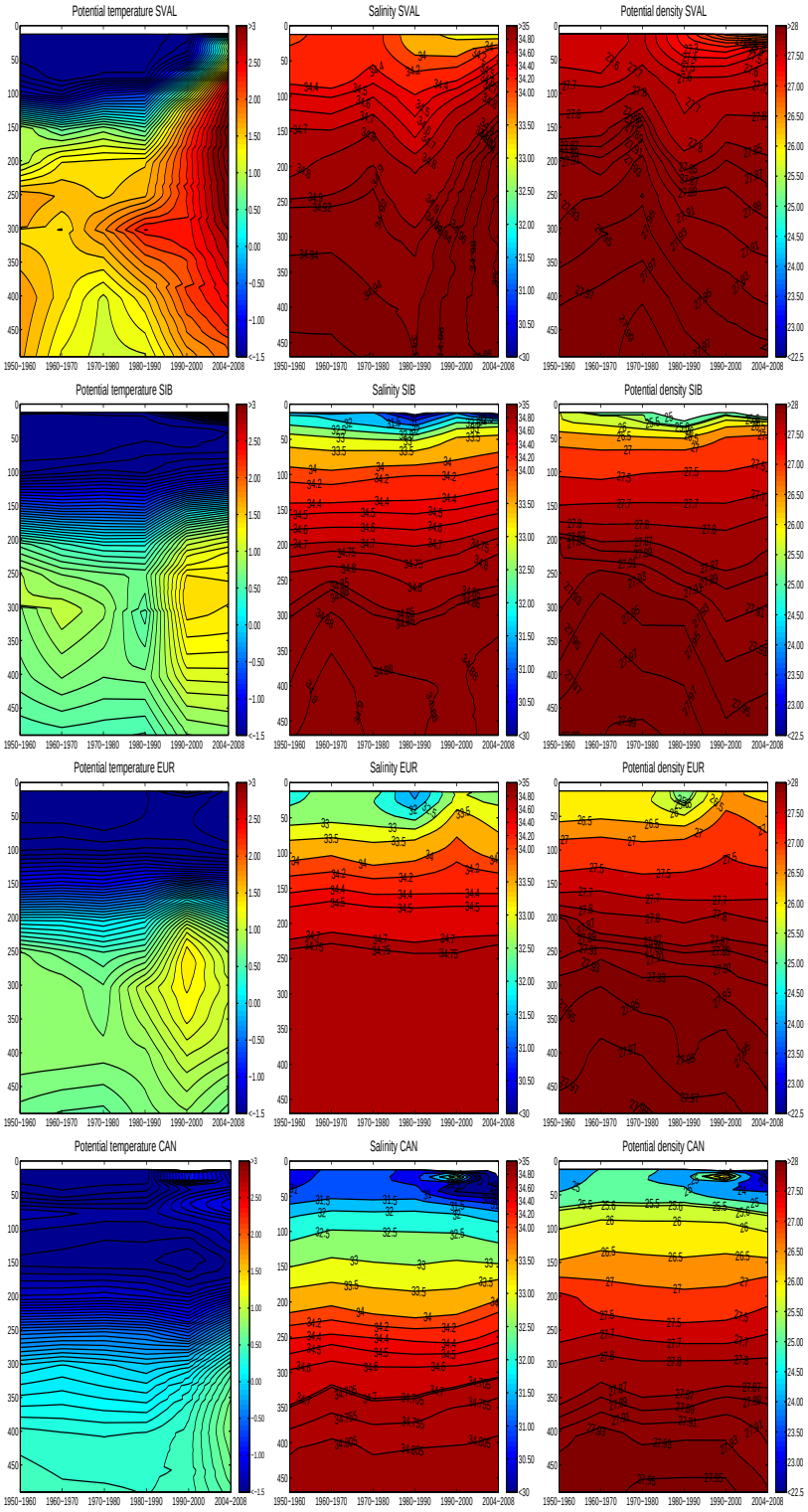

Figure 15: Potential temperature, salinity and potential density Hovmoller diagrams from 1950 till 2008 (decadal data) in the North of Spitsbergen Region (SVAL, upper figures), Laptev Sea (SIB), the Central Eurasian Basin (EUR) and in the Canadian Basin (CAN) (lower figures). NOTE: The vertical resolution in the historical data (1950-1990) is coarse (5db, 25db, 50db and 100 db depending on the depth), whereas the resolution after 1990 is 5 db.

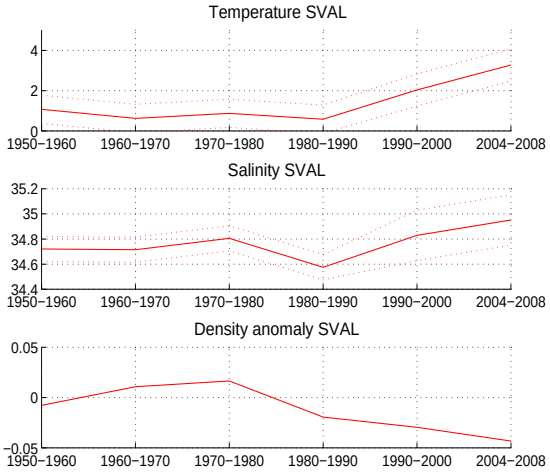

Figure 16: Time series from 1950 til 2008 in the core of the Atlantic Layer (at 200 db) in the north of Spitsbergen region (SVAL, red box), showing potential temperature, salinity and density anomalies. The dotted lines are the error estimates.

but negative in the core of the Atlantic Layer after the 1980s.

Further into the Arctic Ocean, in the **Central Eurasian Basin** (red and blue locations), larger changes in the Atlantic Layer are observed in the 1990s, with decreasing temperatures and salinities going into the 21^{st} century, however the values in the 21^{st} century are still higher than the historical data, as can be seen in figure 18 (time series of temperatures, salinities and density anomalies in the Atlantic Layer). The Atlantic Water temperatures in the 21^{st} century are higher than the 1980s with between 0.2-0.5$\pm$0.4 °C. The temperature anomalies reach 0.5$\pm$0.4 °C in the 21^{st} century. The warming is accompanied by salinification, with salinities 0.2$\pm$0.1 units higher than the 1980s. The density anomalies are small but negative after the 1980s. These findings are in accordance with Richter-Menge et al. (2008), who found that in spring 2007 the core temperature of the Atlantic Water near the North Pole was increased by 0.5 °C above pre-1990s climatology, and results indicate that in 2007 upper-ocean salinity structure and Atlantic Water temperatures in the central Arctic Ocean moved away from climatology, with increased temperatures and salinities.

In the Atlantic Layer on the Canadian Side of the Lomonosov Ridge (green box) the temperatures in the 21^{st} century are higher with up to 0.5$\pm$0.4 °C when compared to the historical data. The temperature anomalies are 0.6$\pm$0.4 °C in the 21^{st} century. The salinities are higher with 0.2-0.4$\pm$0.1 units compared with the historical data. The water in the core of the Atlantic Layer are less dense in the 21^{st} century compared to the EWG data due to the increased temperatures.

In the Beaufort Gyre in the **Canadian Basin** (black box), the Atlantic Water temperatures increased with up to 0.5$\pm$0.4 °C from the 1980s into the 21^{st} century, as shown in figure 19 (black line). The temperature anomalies in the Atlantic

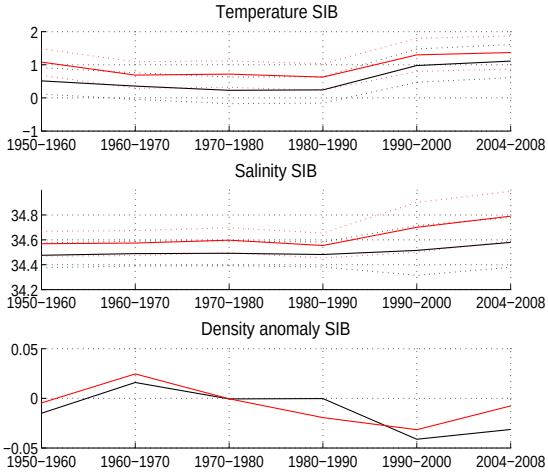

Figure 17: Time series from 1950 till 2008 in the the Atlantic Layer (at 250 db) in two regions (red and black boxes) located near the Laptev Sea (SIB), showing potential temperature, salinity and density anomalies.

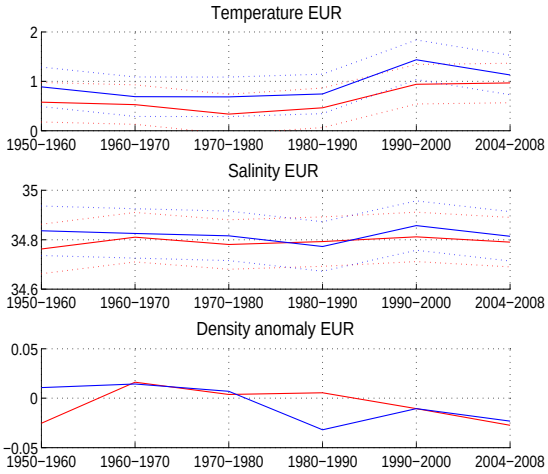

Figure 18: Time series from 1950 till 2008 in the the Atlantic Layer (at 300 db) in the Central Eurasian Basin (EUR, red and blue boxes), showing potential temperature, salinity and density anomalies. The dotted lines are the error estimates.

Layer are up to 0.5±0.4 °C warmer than normal (with normal being the EWG climatology). The salinities in the Atlantic Layer are 0.2 ± 0.1 units higher in the 21^{st} century compared to the 1980s. Below 350 db and down to 500 db the salinity in the 21^{st} century is similar to the historical data, with changes less than 0.04±0.1 units. The density anomalies are small but negative in the core of the Atlantic Layer after the 1990s.
In the Atlantic Layer in the red box north of the Beaufort Gyre in the 21^{st} century (figure 19, red line) the temperatures are higher with 0.1-0.35±0.4 °C and they are therefore not statistically significant. The salinity in the Atlantic Layer has a peak in the 1990s, and going into the 21^{st} century the salinity is decreasing and are at the same values as the historical data, see figure 19. The density anomalies are small but negative in the core of the Atlantic Layer in the 21^{st} century.

These results indicate that the changes in the Atlantic Layer decrease further away from the inflow region, meaning that the hydrographic changes are largest in the region with the highest AWI-indexes. The region north of the Beaufort Gyre (region with the lowest AWI-indexes) has statistically insignificant changes in the Atlantic Layer. The large temperature increase in the region north of Spitsbergen indicates that in the 21^{st} century more heat is lost from the Atlantic Layer to the surrounding ocean than in previous decades. Nevertheless the different rate of heating could also be due to time lag (this is further discussed in chapter 5).

4.2.2 Changes in the Pacific Water

From chapter 4.1 it is clear that three out of the nine boxes have Pacific influence, namely the green box on the Canadian side of the Lomonosov Ridge, and the red and black box in the Beaufort Gyre in the Canadian Basin.
The largest changes in the 1990s and in the beginning of the 21^{st} century in the Pacific Layer are found in the Beaufort Gyre (black box) at depths between 50-100 db. Here the Pacific Water temperatures are between 0.1-0.6±0.425 °C higher in the 21^{st} century compared to the pre-1990s data, shown in figure 20 (black line). The temperature anomalies reach 0.5±0.425 °C, accompanied by a freshening of nearly 1±0.125 unit. The density anomalies are negative after the 1980s due to the warming and strong freshening, with density anomalies down to -1 $\frac{kg}{m^3}$ in the 21^{st} century.
The red box north of the Beaufort Gyre has lower PWI-indexes, and the changes in temperature in the Pacific Layer are not statistically significant in the 21^{st} century compared to the 1980s, see figure 20 (red line). Nevertheless the salinity in the Pacific Layer decreases with more than 1±0.125 unit. The increased temperatures and decreased salinities lead to less dense waters after the 1990s, with density anomalies down to -1 $\frac{kg}{m^3}$.
The green box located on the Canadian Side of the Lomonosov Ridge has no significant changes in the Pacific Water temperature in the 21^{st} century. Also here there is a strong freshening when going into the 21^{st} century, the waters are fresher with up to 1±0.125 unit. The density anomalies are negative after the 1980s due to the warming and strong freshening.
The Pacific Water changes are, as for the Atlantic Layer, largest in the regions

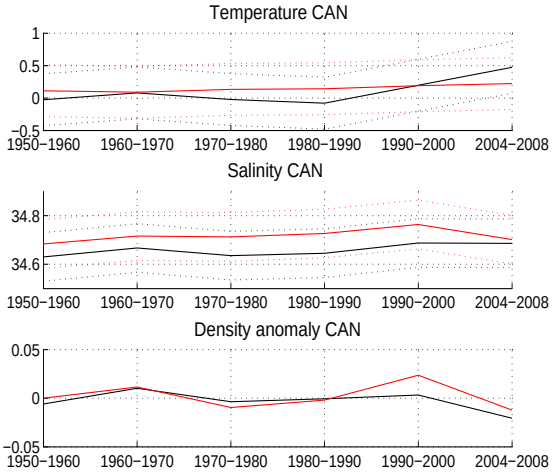

Figure 19: Time series from 1950 till 2008 in the the Atlantic Layer (at 350 db) in the Central Canadian Basin (CAN, red and black box), showing potential temperature, salinity and density anomalies. The dotted lines are the error estimates.

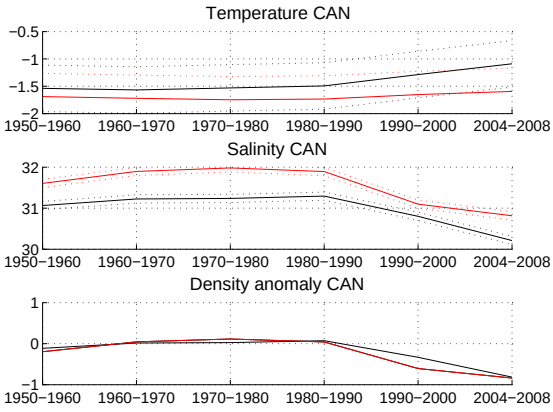

Figure 20: Time series from 1950 till 2008 in the the Pacific Layer (at 50 db) in the Central Canadian Basin (CAN, red and black box), showing potential temperature, salinity and density anomalies. The dotted lines are the error estimates.

closest to the inflow region (in this case the Bering Strait), with insignificant increase in temperature further away from the inflow where the PWI-indexes are smaller.

The hydrographic changes in both the Atlantic and Pacific waters are summarized in figure 21.

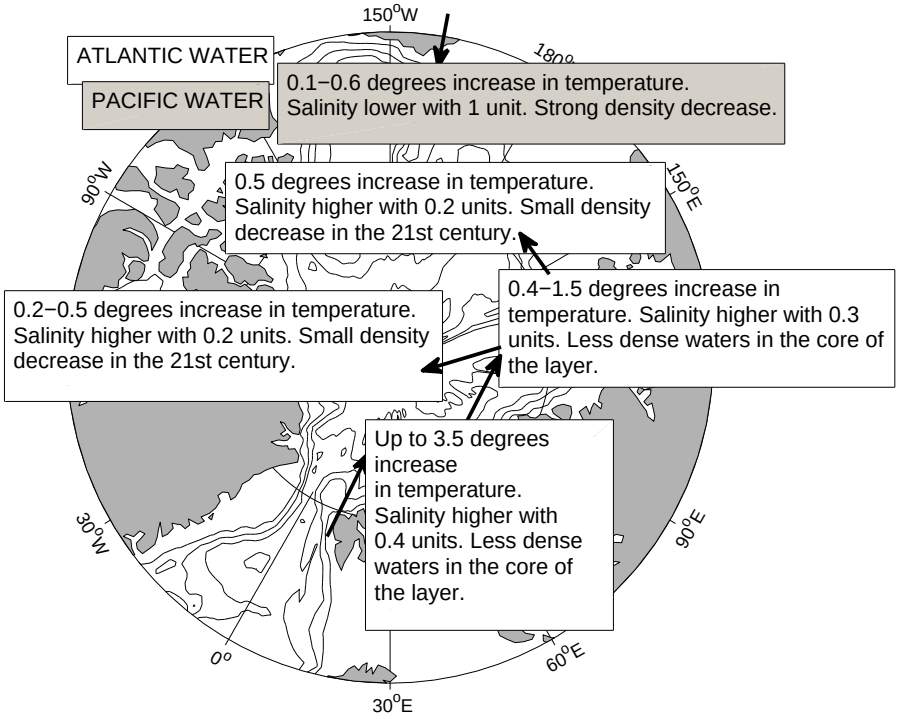

Figure 21: Summary of the hydrographic changes seen after the 1990s in the Arctic Ocean in the Atlantic Water (white) and Pacific Water (gray).

4.2.3 Heat content analyses in the Beaufort Gyre

As we have seen, large changes are observed in the Pacific Layer in the Beaufort Gyre area. The area with the record low sea ice concentrations in the 21^{st} century is an area with high Pacific Influence, namely north of the Siberian and Alaskan coasts (the Western Arctic Ocean). Therefore I wanted to quantify the heat in the Beaufort Gyre area during the years 1996 till 2008 (the temporal and vertical resolution in the EWG was too poor for this analyses, and there were too few observations from 1990-1996), to see if there were significant changes that could be connected with the large changes in the sea ice. These results will be further discussed in chapter 5.
Equation 1 (called the Water Mass Method) was used to estimate the heat budget in a constant volume box in the Beaufort Gyre from 1996-2008 . C_p is the specific heat, that is a measure of the heat energy required to increase the

temperature with 1K per kilo of seawater when the pressure is kept constant. For seawater $C_p = 3985\frac{J}{kgK}$. ρ is the density for sea water, in the calculations $\rho \approx \rho_0 \approx 1028\frac{kg}{m^3}$ is used, where ρ_0 is a constant seawater density. θ_0 is the potential temperature in the given pressure interval, where the freezing point temperature $T_{fr} = -1.910\,^{\circ}\mathrm{C}$ has been subtracted from the initial value.

$$
\begin{aligned}
H_{upper} &= \int_{ML}^{TC} (C_p * \rho * \theta_0(p))\mathrm{d}p \approx \sum_{ML \rightarrow TC} (C_p * \rho_0 * \theta_0(p))\Delta P \\
H_{lower} &= \int_{TC}^{700} (C_p * \rho * \theta_0(p))\mathrm{d}p \approx \sum_{TC \rightarrow 700} (C_p * \rho_0 * \theta_0(p))\Delta P \\
H_{total} &= \int_{ML}^{700} (C_p * \rho * \theta_0(p))\mathrm{d}p \approx \sum_{ML \rightarrow 700} (C_p * \rho_0 * \theta_0(p))\Delta P
\end{aligned} \tag{1}
$$

The Water Mass Method calculates the heat in the upper layers as the heat from the mixed layer (ML) to the start of the thermocline (TC). The heat in the upper layer will therefore give an estimate of the heat in the Pacific water masses in regions with Pacific influence. The heat in the lower layers is calculated as the heat between the thermocline and the 700 db isobar, and will be an estimate of the heat in the Atlantic water masses.
Heat content analysis in the Beaufort Gyre (figure 22) shows that the content of heat in the Pacific Layer (blue line) has increased with approximately $3 * 10^8 \frac{J}{m^2}$, namely from $4.9 * 10^8 \frac{J}{m^2}$ in 1997 to $8 * 10^8 \frac{J}{m^2}$ in 2007. The heat in the bottom layer, that is the Atlantic water masses, has also increased from 1996-2007 with approximately $9 * 10^8 \frac{J}{m^2}$, that is from $8.7 * 10^9 \frac{J}{m^2}$ in 1997 to $9.6 * 10^9 \frac{J}{m^2}$ in 2007. 2007 has the maximum amount of heat in this 12 years period, and 2007 is also the year with the record low sea ice extent. The maximum amount of heat in the Pacific Layer in 2007 could be due to increased heat uptake from the atmosphere to the ocean due to decreased albedo. Another option is that the ocean warmed independently of the atmospheric temperatures, and led to an increased heat flux in the upper ocean enhancing the sea ice melting. These options are further investigated in chapter 5.

4.3 Changes in the depth of the upper interface between Halocline Water and Atlantic Water

It turns out that not only are there significant changes in temperature, salinity and density, but there are systematic changes in the depth of the upper interface between the Atlantic Water and the above-lying Halocline Water. Presently the warm Atlantic Water cannot affect the Arctic sea ice significantly because the warm water is covered by a thick layer of cold water. As the Atlantic Water runs more shallow, the cold halocline layer is thinning and the sea ice is more exposed to the warm Atlantic Water.
To study this I defined the upper interface between the Halocline Water and Atlantic Water as the $0\,^{\circ}\mathrm{C}$ isotherm. This is the same definition as used in the EWG-atlas. Note that when this definition is used, the cooler Atlantic Water that enters the Arctic Ocean through the northern Kara Sea will not be identified as Atlantic Water (Dmitrenko et al., 2008). The data in the EWG atlas were

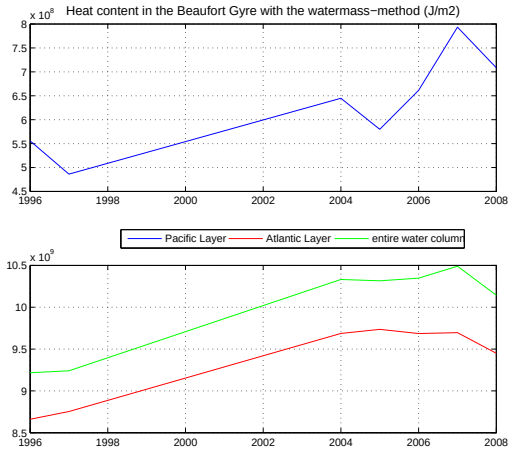

Figure 22: The time evolution of the heat in the Beaufort Gyre area from 1996-2008 in the Pacific Layer (top, blue line), in the Atlantic Layer (bottom, red line), and the total amount of heat from the surface down to 700 db (bottom, green line).

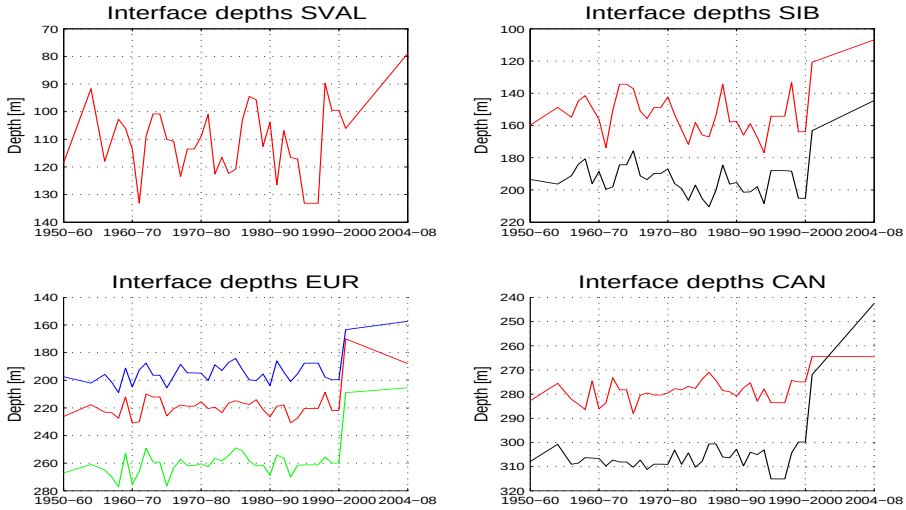

Figure 23: The mean interface depth between the cold halocline layer and the Atlantic Water from 1950-2008, north of Spitsbergen (SVAL) (red box), in the Laptev Sea in the Siberian Continental Shelf area (SIB) (red and black boxes), in the Eurasian Basin (EUR) (red, blue and green boxes, located close to the Lomonosov Ridge) and in the Beaufort Gyre area in the Canadian Basin (CAN) (black and red boxes). Annual data up to 1989, then 10 or 5 years averaged data due to sparseness in the data cover.

annual data. Since my data from 1990-2008 is limited I averaged all years from 1991-2000 to represent the 1990s, and all years from 2004-2008 to represent the state of the art. For the regions north of Spitsbergen and near the Siberian Continental Shelf Area I assumed depths shallower than 40 meters and deeper than 500 meters to be outside the range of the upper interface depth. I assumed that the interface depth was found between 100 and 700 meters in the Central Eurasian and Canadian Basins. Figure 23 shows the changes in the depth of the upper interface from 1950-2008.
In the region **north of Spitsbergen** (SVAL) the interface depth has large year to year variability of approximately 20-30 meters. The interface depth lies at record shallow depths in the early 1990s and in the 21^{st} century, namely 80 ± 10 meters.
The Laptev Sea in the **Siberian Continental Shelf Area** (SIB) has 20 meters year to year variability. The black box has interface depths between 180 and 200 meters from 1950-1990. In the 1990s the interface ascended to 160 meters, and continued to ascend to approximately 140 meters in the 21^{st} century, namely an ascent of approximately 50 ± 10 meters. The red box has interface depths at 140-160 meters in the historical data. The interface lies approximately 40 ± 10 meters more shallow in the 21^{st} century: in the 1990s the interface ascended to 120 meters, and continued to ascend with approximately 10 meters (to 110 meters depth) in the 21^{st} century.
The three locations in the **Central Eurasian Basin** (EUR) show an ascending trend in the interface depths when going into the 1990s. The interface depth in the historical data was fairly constant, whereas the interface dropped off approximately 50 ± 10 meters from the 1980s till the 1990s. However there is no further ascent when going into the 21^{st} century, the red box has a small *descent* towards the pre-1990s level, however the interface depth is still shallower than the historical data with approximately 30 ± 10 meters.
The black box in the Beaufort Gyre in the **Canadian Basin** (CAN) has interface depths at approximately 300-310 meters from 1950-1990. In the 1990s the interface has ascended to 270 meters, an ascent of 30 ± 10 meters. The interface continues to ascend with 30 ± 10 meters in the 21^{st} century, meaning that the interface lies at approximately 240 meters. The red box has interface depths at approximately 280 meters in the historical data, going into the 1990s the interface is 15 ± 10 meters above climatology, and there is no further ascent in the 21^{st} century.

These results indicate that the Atlantic Water runs more shallow compared to the historical data in all of the regions investigated in the 21^{st} century. The ascent started in the 1990s, before that there were no large changes in the interface depth in the Canadian and Eurasian Basins, whereas there was larger year to year variability north of Spitsbergen and also in the Siberian Continental Shelf Area. However the Atlantic Water runs more shallow than ever monitored in the 21^{st} century in these regions as well. The changes are summarized in figure 24.

4.4 Pulses and/or trends?

Since the inflow of warm Atlantic Water to the Arctic is characterized by large warm pulses it is difficult to see whether there really is a long term warm-

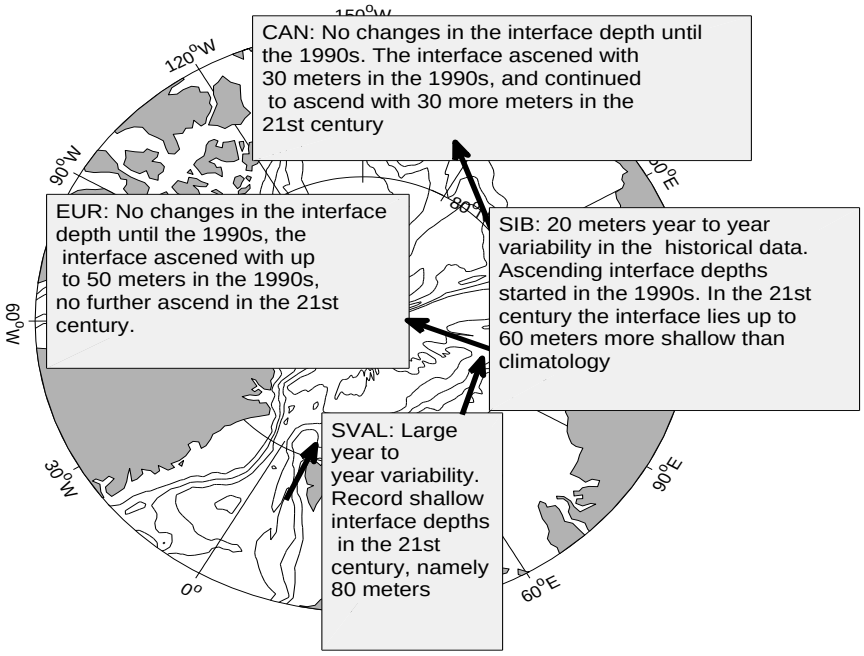

Figure 24: Summary of the observed changes in the interface depth in the 21^{st} century compared to the historical data.

ing trend. Grotefendt et al. (1998) concluded that the warming they observed in the 1990s could **not** be attributed to a climatic trend but rather to decadal fluctuations, which appeared to be connected to the NAO/AO-circulation regimes. However the warming of the Arctic Ocean accelerated even though the NAO/AO-index decreased in the 21^{st} century, as shown in chapter 2.1.3. However Dmitrenko et al. (2008) suggested that the Arctic Ocean is going towards a new, warmer state, since the anomaly magnitude exceeds the level of pre-1990 mean.
In chapter 4.4.1 earlier widespread Atlantic Layer changes are investigated, to see if the changes seen in the 1990s and in beginning of the 21^{st} century are unique. In chapter 4.4.2 warm pulses after the 1990s are localised to find out whether the changes seen in recent decades are connected to warm pulses, or if they are a long term trend with the pulses superimposed on this trend.

4.4.1 Atlantic Layer changes from 1950 till 1995

I wanted to find out if the changes seen in the 1990s and in the 21^{st} century were the largest ever observed, or if the underestimation of variability in the historical data set was too large for detecting earlier changes. The salinity, potential temperature and potential density fields are 10 years averaged in the EWG atlas and therefore variability is underestimated since inter-annual variability can not be detected. Swift et al. (2005) have developed a data set with annual resolution to detect variability in the EWG data set. They wanted to determine whether there had been earlier widespread Atlantic Layer changes

similar to those seen in the 1990s. Figure 25(a) is from the article 'Long-term variability of the Arctic Ocean waters: Evidence from a reanalyses of the EWG data set' written by Swift et al. (2005). The figure shows an annual averaged Hovmoller temperature diagram covering a region north west of the Laptev Sea. I have compared this result with results derived from the original EWG decadal averaged data set. The original decadal data show that this is an unusual region regarding the variability in temperature. The decade to decade variability is larger than any other box investigated. Figure 25(b) is the reproduced figure from Swift et al. with the original decadal data set.

High temperatures are found in the 1950s with the original EWG decadal data, with temperatures reaching 1.38 °C. The annual data from Swift et al. shows a maximum temperature in 1953 with temperatures in the Atlantic Layer reaching 1.7 °C, however the Atlantic Water during the rest of the 1950s is approximately 1.3 °C. From the early 1970s till the 1990s the annual data show decreasing temperatures in the Atlantic Layer, and increasing temperatures in the 1990s with temperatures between 1.46 °C and 1.7 °C. The original EWG data set shows a strong temperature increase from the 1990s and going into the 21^{st} century the temperatures are up to 1.46 °C.

Therefore the variability in the EWG decadal data set is comparable to the annual variability reproduced by Swift et al., although the variability is less in the original EWG data set. The original data set suggests that the changes seen after the 1990s are a trend towards higher temperatures. The observed changes in recent decades are the largest changes ever observed, and this is not due to underestimation of variability in the historical data.

4.4.2 Warm pulses after the 1990s

To see the extent and duration of warm pulses after the 1990s temperature anomalies from 1990-2008 (annual data) were calculated by using the EWG-climatology as reference values. Negative anomalies imply lower temperatures than the historical EWG data set (from 1950 to 1990), whereas positive anomalies imply temperatures above climatology. Note that the vertical resolution in the EWG data set is poor (since the only depths with hydrographic data in the EWG data set are 5m, 10m, 25m, 50m, 75m, 100m, 150m, 200m, 250m, 300m, 400m and 500m). Also the annual resolution in the data from 1990 till 2008 century is sparse in some of the regions investigated. Nevertheless figure 26 shows the extent and duration of anomalies in the Arctic Ocean, for the north of Spitsbergen region (SVAL) (upper figure), the Laptev Sea area (SIB), the Eurasian Basin (EUR) and the Canadian Basin (CAN) (lower figure). Negative anomalies are plotted in white.

Figure 26 shows that the Atlantic Layer is almost always warmer than the 1950-1990 average. In addition there are years where so called warm pulses are present. The arrows suggest a possible propagation of two warm pulses through the Fram Strait, one in the beginning of the 1990s (as found by Quadfasel et al. (1991)), and one in the beginning of the 21^{st} century (as found by Karcher et al. (2003) and Dmitrenko et al. (2008)). The first warm pulse has reached the Laptev Sea area by 1996 (approximately 3 years lag), the Eurasian Basin by 1999 (6 years lag) and the Canadian Basin by 2004/2005 (11 till 12 years lag). Shimada et al. (2004) found that the warm anomaly from the Fram Strait Branch was observed on the eastern flank of the Northwind Ridge south

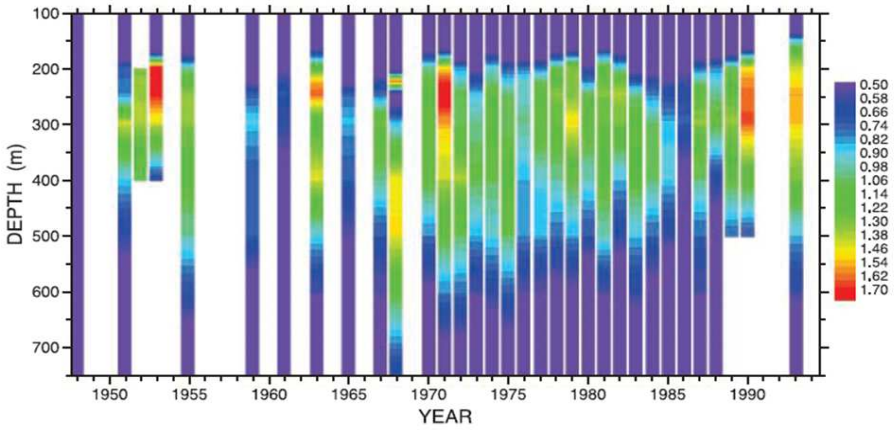

(a)

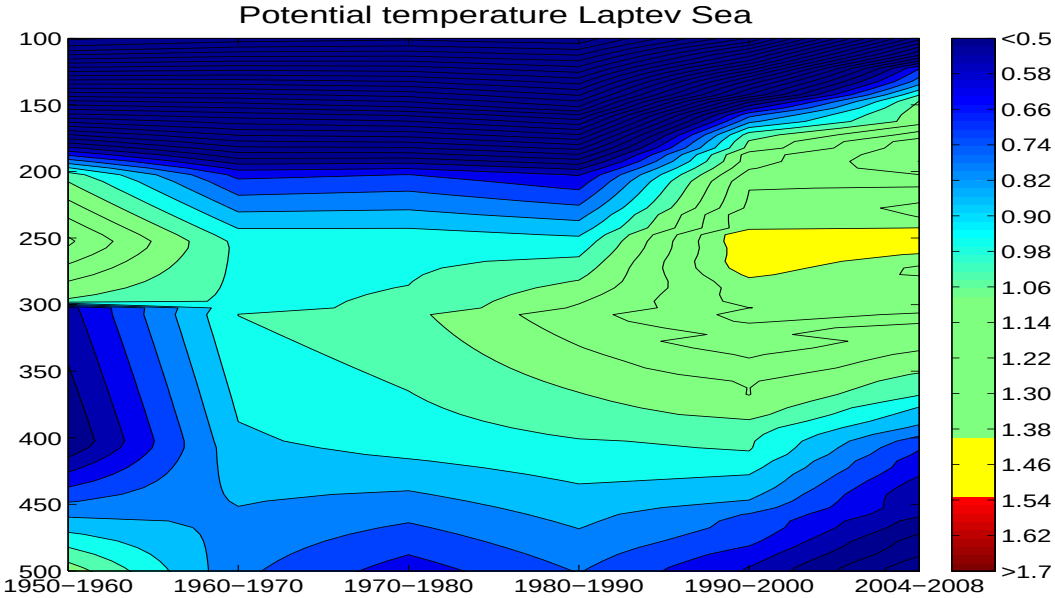

(b)

Figure 25: (a): The Atlantic Layer annual average (from 1950-1995) temperature profiles for a box north west of the Laptev Sea, from Swift et al. (2005), from a reanalysis of the EWG data set. (b): The decadal time series (1950-2008) made from the original decadal EWG data set for the same region. Waters in the depth range colder than 0.05 °C are colored uniform with the color corresponding to 0.05 °C.

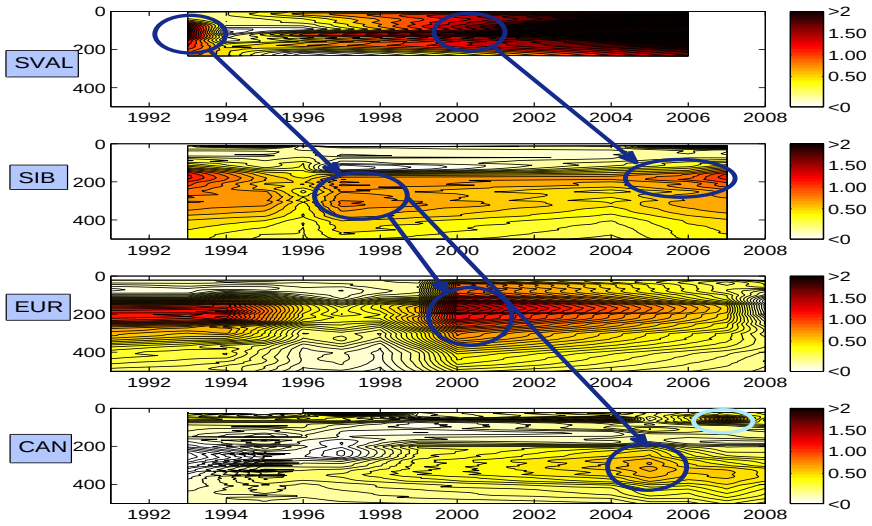

Figure 26: Warm pulses in the Arctic Ocean after the 1990s north of Spitsbergen (SVAL) (upper figure), in the Laptev Sea (SIB), Eurasian Basin (EUR) and Canadian Basin (CAN) (bottom figure) from 1991-2008. Negative anomalies are plotted in white. The arrows suggest a possible propagation of two warm pulses through the Fram Strait (1991 and 2000). The light blue circle at shallow depths in the Canadian Basin indicates anomalously warm Pacific Water in 2007.

of 76 ° north in 2002-2003, which is in good accordance with these results.
The second warm pulse has reached the Laptev Sea area by 2004/2005 (4 till 5 years lag). Dmitrenko et al. (2008) found that the warm anomaly that was present in the Fram Strait in 1999-2000 was found in the Laptev Sea from 2002-2005, which indicates a 3 till 6 years lag between the two regions, which are in good accordance with these lags. One of their mooring positions north of the Laptev Sea showed an abrupt warming of 0.4 °C in February 2004, and a second abrupt warming in August 2005. In February 2005 they found no further temperature increase, however my results extend till 2007, and they show a larger warming in 2006 than ever monitored.
In the Pacific Layer in the Canadian Basin the largest warm anomalies are seen in 2007 ($+0.7\,^{\circ}$C), and also in 2004. Nevertheless the anomalies are positive in all years investigated. The warm event in 2007 are investigated further in chapter 5.
Dmitrenko et al. (2008) found that the anomaly mean velocity speed was $2.4 - 2.5 \pm 0.2 \frac{cm}{s}$. Therefore, if we assume that the observed pulses in the Atlantic Layer travel with the speed $2.4 \frac{cm}{s}$ and that the approximate distance between the north of Spitsbergen region and the Laptev Sea is approximately 2500 km, the travel time is approximately 3 years. Further from the Laptev Sea to the North Pole area, the approximate distance is 2000 km, meaning that the travel time from the inflow region to the Eurasian Basin is approximately 6 years,

which is in good agreement with my results. Further, from the Laptev Sea to the Beaufort Gyre we find that the approximate distance is 7500 km, which implies approximately 13 years lag from the inflow region to the Canadian Basin. These simplified calculations suggest that the pulses on figure 26 have realistic propagation speeds. If the results are correct we would expect to see the early 21^{st} century anomaly in the Eurasian Basin by 2010. In the early 1990s there was unusually warm water in the Laptev Sea, and also in the Eurasian Basin near the Lomonosov Ridge (as found by Karcher et al. (2003)), however at the same time negative anomalies are seen in the Canadian Basin.

To summarize, at depths corresponding to the Atlantic Layer and Pacific Layer there are positive anomalies in almost all years from 1990 till present, and the anomalies are mainly larger in the 21^{st} century than in previous years. There are events of warm pulses in the Arctic Ocean in the Atlantic Layer, and also in the Pacific Layer in the Canadian Basin. The anomalies follow the Arctic circulation upstream. The results imply that warm pulses are superimposed on a long term warming trend rather than being the main signal.

4.5 Verification of the NCAR and UK Met Office HADLEY models

Here I compare observations with results given by the IPCC-models NCAR_CCSM3_0 (National Center for Atmospheric Research) and UK Met Offices HADLEY (UKMO_HADCM3), to see how well the models calculate the observed changes in the beginning of the 21^{st} century, both in ocean potential temperature and Atlantic interface depths (chapter 4.5.1) and in sea ice concentrations and spatial distribution (chapter 4.5.2). The models are two of the global climate models used by the Intergovernmental Panel on Climate Changes (IPCC) in their assessment of the status of understanding the climate changes. They are coupled atmosphere-ocean general circulation models. The spatial resolution in the HADLEY model is $2.5^\circ \times 3.75^\circ$, whereas the resolution in the NCAR model is $1.4^\circ \times 1.4^\circ$.
The potential temperature fields are monthly averaged, whereas the sea ice concentrations are averaged for September and January, and also annual averages are estimated. The IPCC model results for the NCAR and HADLEY models were downloaded from the World Climate Research Program's (WCRP's) Coupled Model Intercomparison Project phase 3 (CMIP3) multi-model dataset (The CMIP3 archive, 2004). For the 19^{th} and 20^{th} century the 'Climate of the 20^{th} century experiment' (20c3m) is used, whereas the A2 experiment is used for the 21^{st} century. The A2 scenario describes a more divided world with a high population growth together with slow technological changes (CCCma, 2005). The emissions are also higher than today. The A2 experiment is the scenario with the largest concentrations of both CO_2 and SO_4. Figure 27 (Raupach et al. (2007)) shows the CO_2 IPCC emission scenarios. The A2 scenario used for the 21^{st} century run in this chapter is the turquoise colored line. The observed CO_2 emissions in the beginning of the 21^{st} century (black lines) are so far larger than any of the scenarios. The CO_2 concentrations reach values above 800 ppm at the end of the 21^{st} century with this experiment (whereas today's value is approximately 380 ppm).

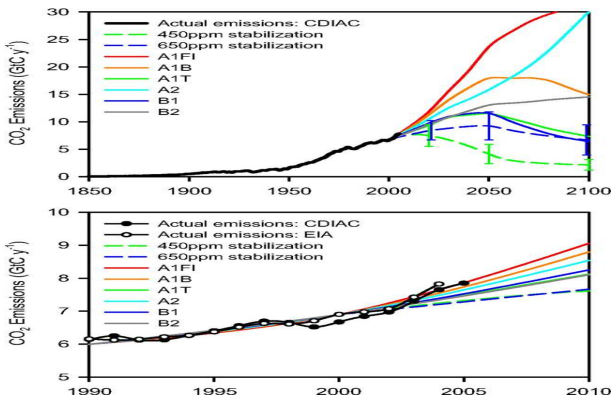

Figure 27: The IPCC scenarios CO_2 emissions. The observed CO_2 emissions (black line) are larger than any of the scenarios. The figure is from Raupach et al. (2007).

4.5.1 Modelled Atlantic interface depths and temperature

The observed interface depths between the cold Halocline Water and warm Atlantic Water, and observed potential temperatures were compared with the HADLEY and NCAR model results in the **Beaufort Gyre area** (figure 28) and in the **Laptev Sea** (figure 29).

In the **Beaufort Gyre area** (figure 28) both models have too shallow interface depths between the halocline waters and Atlantic waters, however the ascending interface after the 1990s are well represented in the NCAR model results. The *observed* upper interface depths between the halocline layer and Atlantic Layer are approximately 300 meters in the historical data, whereas the interface ascended with approximately 60 meters going into the 21^{st} century, as shown in chapter 4.3. The NCAR model's interface lies at approximately 100 meters up to the 1990s, and ascends with approximately 50 meters going into the 21^{st} century, the ascent is in good accordance with the observations. There are no significant changes in the interface depths in the HADLEY model going into the 21^{st} century.

The models estimated temperatures in the Atlantic Layer in the Beaufort Gyre are too high compared to the observations. However the observed warming in the Atlantic Layer in the 1990s is well represented in the NCAR model. The *observations* show that the temperature in the pre-1990s were approximately 0.4 °C in the core of the Atlantic Layer, and the temperatures increased to 0.8 °C in the 21^{st} century, namely an increase of 0.4 °C. The NCAR model has temperatures in the core of the Atlantic Layer at approximately 1.5 °C before the 1990s, in the 21^{st} century the temperatures are up to 1 °C higher. There are no significant changes in temperature in the HADLEY model going into the 21^{st} century.

In both the NCAR and HADLEY models the Atlantic Water temperatures in the **Laptev Sea** (figure 29) are *colder* than in the Beaufort Gyre, meaning that the circulation of Atlantic Water can not be well represented in either of the models. However the temperatures and interface depths are in better accordance with the observations than they were in the Beaufort Gyre. The *observed*

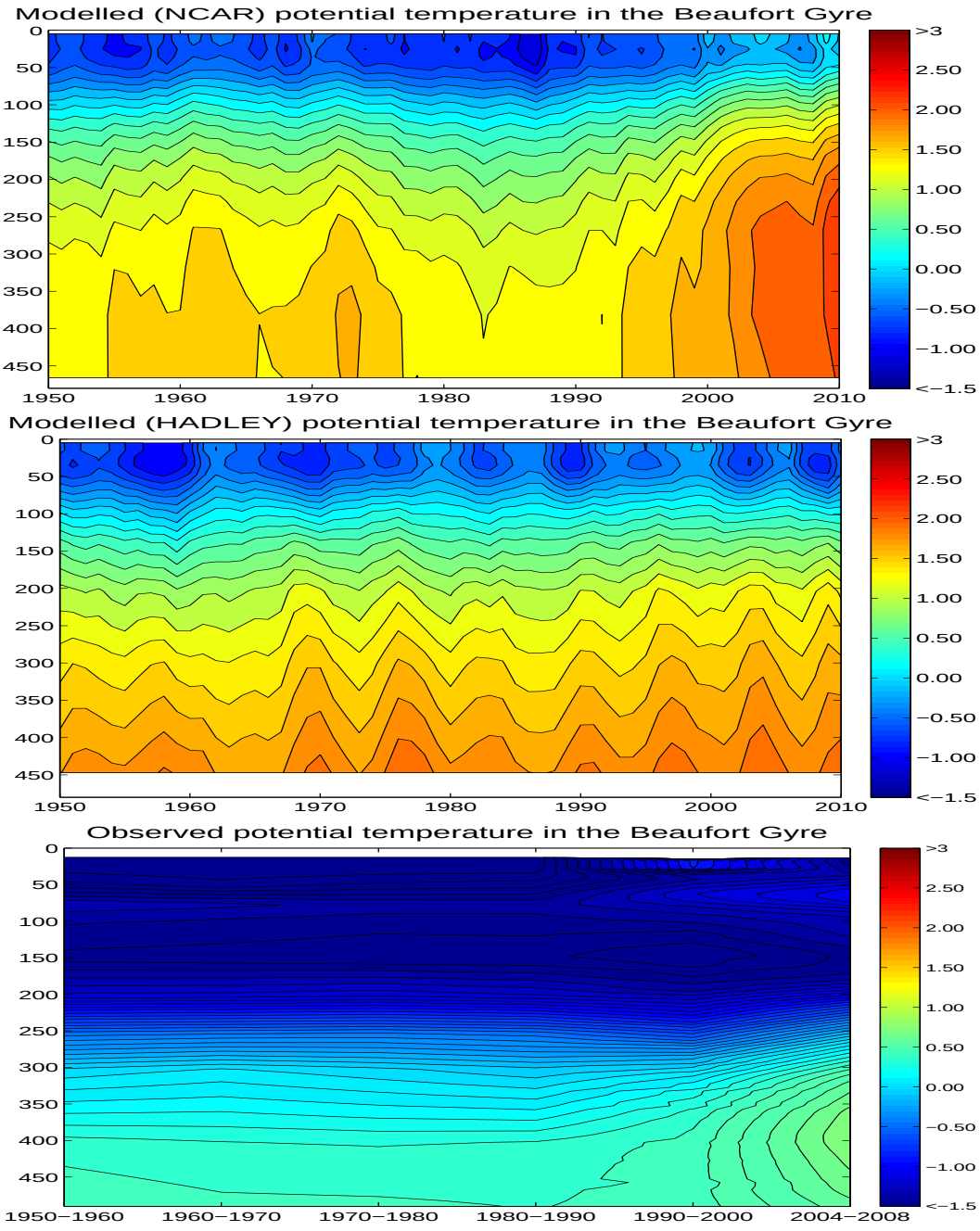

Figure 28: Potential temperature for the NCAR and HADLEY models (annual mean) compared to observations (decadal mean) from 1950-2008 in the Beaufort Gyre.

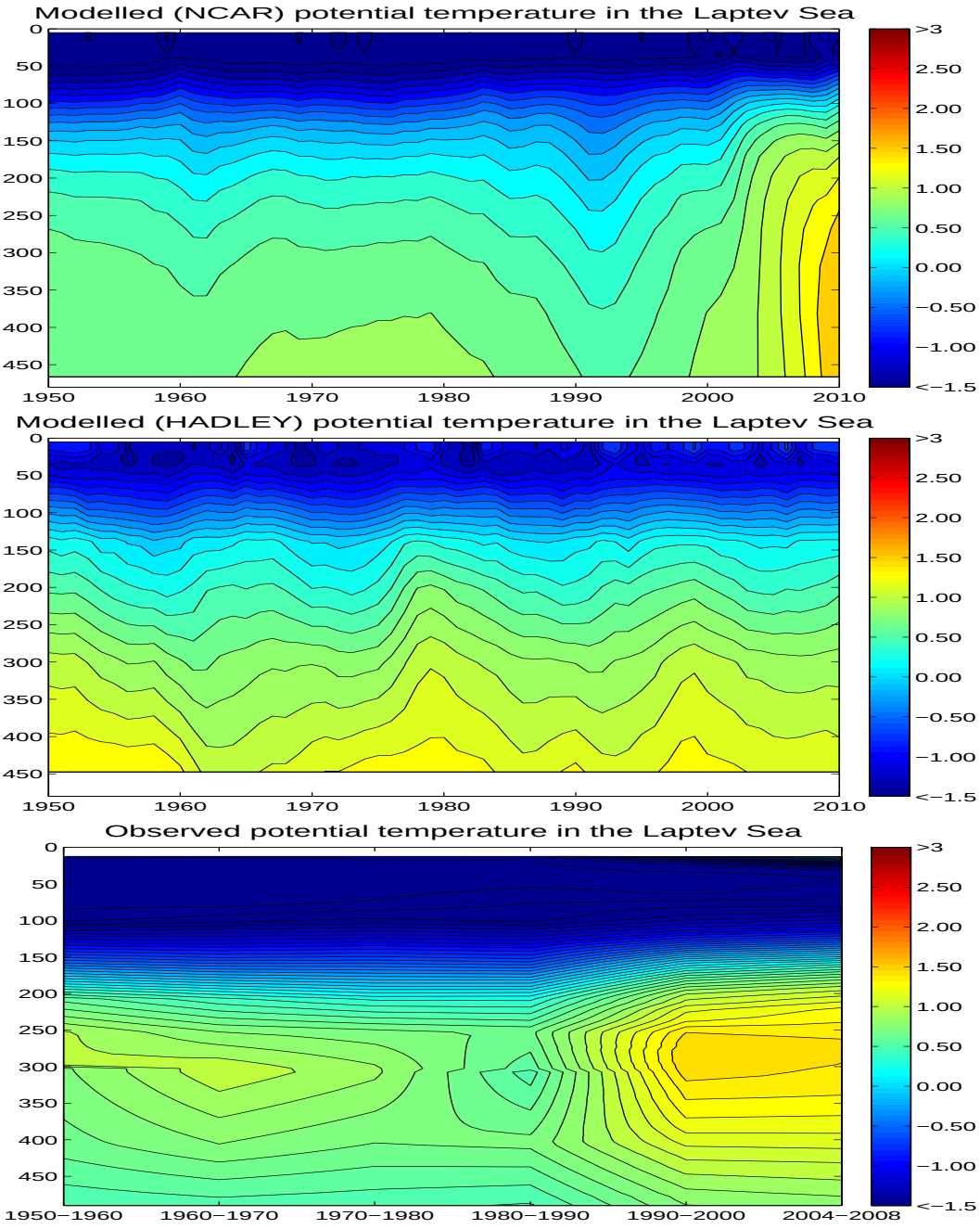

Figure 29: Potential temperature for the NCAR and HADLEY models (annual mean) compared to observations (decadal mean) from 1950-2008 in the Laptev Sea.

interface depths between the Halocline Water and Atlantic Water are approximately 200 meters up to the 1990s, and going into the 21^{st} century the interface ascends with up to 60 meters, as shown in chapter 4.3. The NCAR model has interface depths at approximately 150 meters before the 1990s, after that the interface ascends with approximately 50 meters, which is in good accordance with the observations. The HADLEY model has interface depths at approximately 100 meters, but the ascending trend is not represented in the model result.
NCAR is in good accordance with the observed temperature changes when going into the 21^{st} century. In the NCAR model the temperature in the core of the Atlantic water masses increases with 0.75 °C in the 21^{st} century, namely from 1 °C before the 1990s to 1.75 °C in the 21^{st} century. The *observed* changes when going into the 21^{st} century are up to 1.5 °C warmer than the historical data. There are no significant changes in temperature in the HADLEY model going into the 21^{st} century.

4.5.2 Modelled sea ice extent and spatial distribution

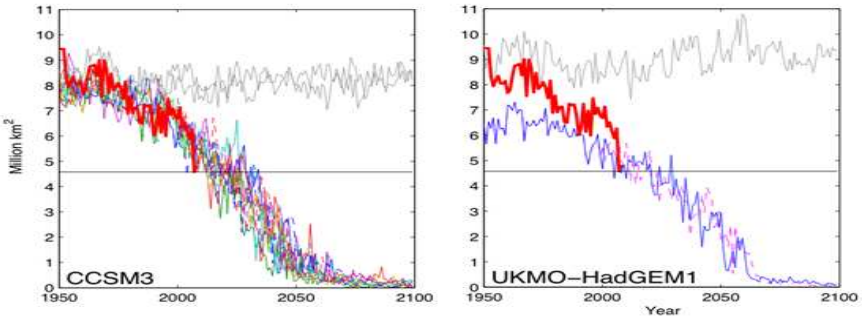

Figure 30: September sea ice extent from 1950-2100 with the NCAR (left) and HADLEY (right) models compared to observations (red line) from Wang and Overland (2009). The gray line indicates a control run with no further CO_2 increase. The control runs show that anthropogenic forcing is necessary for the large sea ice loss at the end of this century.

When comparing the models sea ice extent with the observed sea ice extent at the end of the 20^{th} and in the beginning of the 21^{st} century NCAR has the most realistic sea ice cover. The simulated sea ice extent is in good accordance with the observations, and also the negative trend at the end of the 20^{th} and in the beginning of the 21^{st} century is well reproduced. The HADLEY model has a stronger overestimation of the sea ice extent compared to observations, however the negative trend is well reproduced. This is shown in figure 30 from Wang and Overland (2009) (left figure is NCAR and right figure is HADLEY). The red line is the observations, and the gray line indicates control runs with no further CO_2 increase. The control runs show that anthropogenic forcing is necessary for the large negative trend in sea ice extent, this is discussed further in chapter 5.4.
The observed sea ice extent in the 21^{st} century was especially low in the area

north of the Siberian and Alaskan coasts, that is in the Western Arctic Ocean, as shown in figure 1(a). By comparing the observed and modelled spatial distribution of the sea ice I found that the spatial distribution in the models are not correct. There are too much ice in the Canadian Basin in both models, and also too much ice in the HADLEY model around Spitsbergen. The coarse model resolution compared to observations limits the models spatial accuracy. Nevertheless the observed trends with decreasing sea ice cover are well reproduced in both models.

To summarize: The NCAR model reproduces the changes seen after 1990 fairly well, both the warming and lifting of the Atlantic Layer and the decrease in sea ice extent are fairly reproduced. The negative trend in sea ice extent is also fairly reproduced in the HADLEY model, however changes in temperature at the end of the 20^{th} and in the beginning of the 21^{st} century are too small.

5 Discussion

In this chapter possible connections between the ocean and sea ice are discussed. In chapter 5.1 the Atlantic Layer influence is discussed, the Pacific Layer influence is discussed in chapter 5.2. In chapter 5.3 the future predictions from the NCAR and HADLEY models, in potential temperature and sea ice concentration, are analyzed. The importance of anthropogenic emissions for the modelled changes in ocean temperature and sea ice concentrations is discussed in chapter 5.4.

5.1 Atlantic Layer influence

Large changes in both temperature, salinity, density and in the heat content are observed in the 21^{st} century. The large changes started in the 1990s, and continued to increase going into the 21^{st} century almost everywhere in the Arctic Ocean. Traditionally it has not been argued in favour of a close relationship between the Atlantic Layer and the sea ice extent because of the halocline layer, that lies as a cold protective interface above the Atlantic Water. However heat is lost as the Atlantic Water is transported throughout the Arctic Ocean. The Atlantic Layer runs more shallow in recent decades compared to the EWG atlas, meaning that the thick cold halocline layer is thinning, and the Atlantic influence to the overlying ocean gets more and more important as the interface continues to ascend. The largest changes in the Atlantic temperatures in the 21^{st} century are observed in the inflow region north of Spitsbergen, whereas the Eurasian and Canadian Basins have remarkably smaller changes. Since these parts of the Atlantic Layer have not been heated with the same speed as the inflowing waters, it could imply that more heat is now lost from the Atlantic Layer to the surrounding ocean. The increased heat loss from the Atlantic Water in the Arctic must sooner or later contribute to change the energy balance up towards the sea ice. However from chapter 4.4.2 we find that the time lag between the inflow region and the Canadian Basin is more than 10 years, which could imply that the difference in warming is associated with time lag. Whether there is increased heat loss from the Atlantic Water or if the

differences in warming are due to slowness in the system needs more investigation.
In absence of the cold halocline layer, is there enough heat within the Atlantic Layer to significantly influence the sea ice cover? We can do a back-on-the-envelope estimate on what amount of heat must be added to the sea ice to reduce the thickness of it with approximately 1 meter in 20 years, that is the approximate observed melting. The heat content (HC) needed to melt m kilos of ice is in one year is:

$$HC = m * L \leftrightarrow Q * A \approx \rho_{ice} * A * D * L \tag{2}$$

,where the heat content is $HC \approx Q * A$, where A is the area of the sea ice cover (m^2) and Q is the heat transport given in $\frac{W}{m^2}$. ρ_{ice} is the density of the ice, approximately $900\frac{kg}{m^3}$, D is the change in thickness of the sea ice with time ($\frac{m}{s}$) and L is the latent heat of ice ($3.35 * 10^5 \frac{J}{kg}$). Equation 2 gives us:

$$Q \approx \rho_{ice} * D * L \tag{3}$$

We assume that the sea ice cover in the Arctic is thinner with 1 meter in 20 years, meaning that $D = 0.05\frac{m}{year} = 1.6 * 10^{-9}\frac{m}{s}$. This gives us:

$$Q \approx \rho_{ice} * D * L \approx 900\frac{kg}{m^3} * 1.6 * 10^{-9}\frac{m}{s} * 3.35 * 10^5 \frac{J}{kg} \approx \underline{0.5}\frac{W}{m^2} \tag{4}$$

The result implies that to melt 5 cm ice in one year, if the energy is only used for this purpose, you need an extra heat flux of 0.5 $\frac{W}{m^2}$. The results from this simple scaling are in good accordance with Polyakov et al. (2004) who estimated that the 0.8-1.0 meters loss in ice thickness over the last 20 years represented a heat flux with an amplitude of $0.4 - 0.6\frac{W}{m^2}$.

With a back-of-the-envelope estimate of the equation of conservation of heat (equation 5), it is possible to quantify the magnitude of the heat flux from the Atlantic Layer to the surrounding ocean. We assume a simple box model, a stream tube of Atlantic Water, with equal masses flowing in (warm water) and out (cooled water) of the Arctic Ocean. We assume that the temperature of the inflowing waters (θ_{in}) is 3 °C, whereas the temperature of the outflowing waters (θ_{out}) is 1 °C (Dmitrenko et al., 2008). The area A in our box equals the total area of the Arctic ($A_{tot} = 9.5 * 10^{12} m^2$ (Knauss, 2005)). For this simple scaling we assume that the volume transport of Atlantic Water in and out of the Arctic equals 7.1 Sv (that is $7.1 * 10^6 \frac{m^3}{s}$), adapted from Talley et al. (2009), as an estimate of the volume transport in the West Spitsbergen Current. This is of course a simplification, this approach eliminates the heat from the Barents Sea branch into the Arctic Ocean, nevertheless for this simple scaling we will assume this.

The equation of conservation of heat is:

$$\frac{\delta\theta\rho}{\delta t} + \nabla \cdot \rho\theta\overrightarrow{u} = S * \delta A \tag{5}$$

The first term on the left hand side is the time derivative, the change in temperature with time. The second term is the advection part of the equation, the change in temperature as heat is transported with the flow. θ is the ocean potential temperature, ρ is a constant density of sea water ($1028\frac{kg}{m^3}$), and $\overrightarrow{u}$ is the three dimensional velocity vector. S is an exchange of heat term, namely $\frac{Q}{C_p}$, where C_p is the specific heat ($C_p = 4000\frac{J}{kgK}$) and Q is the heat transport given in $\frac{W}{m^2}$.
It would simplify the equation if we could assume that the system was in steady state, meaning that the temperature is not changing in time. However in this theses I have shown that the system *is* changing in time. The observed changes are significant in *some* parts of the Arctic, however the largest part of the Atlantic Water has not been heated with the same speed. We do a simple scaling on the left hand side of equation 5, to see which term has the dominating size. We use Gauss theorem on equation 5.

$$\frac{\delta\theta\rho}{\delta t} \rightarrow \frac{\delta}{\delta t}\iiint \rho\theta\delta V \sim \frac{\rho\delta\theta * V}{t} \tag{6}$$

$$\nabla \cdot \rho\theta\overrightarrow{u} \rightarrow \iiint \nabla \cdot \rho\theta\overrightarrow{u}\,\delta V = \oint\oint \rho\theta\overrightarrow{u} \cdot \overrightarrow{n}\,\delta A \sim$$
$$(\rho_{in} * \theta_{in} * u_{in} * A_{in} - \rho_{out} * \theta_{out} * u_{out} * A_{out}) \tag{7}$$

V is the volume of the Atlantic water masses that has heated in recent decades, and $\frac{\delta\theta}{t}$ is the speed of the heating, let us assume that the waters are warmer with 1 °C per 20 years. We assume conservation of mass, that is:

$$\begin{aligned} \iiint \nabla \cdot \overrightarrow{u}\,\delta V &= 0 \\ \Leftrightarrow \oint\oint \overrightarrow{u} \cdot \overrightarrow{n}\,\delta A &= 0 \\ \Leftrightarrow u_{in} * A_{in} &= u_{out} * A_{out} \end{aligned} \tag{8}$$

When adding equation 7 and 8, and assuming that $\rho_{in} = \rho_{out} = \rho$, the advection term can be scaled as:

$$\rho_{in} * \theta_{in} * u_{in} * A_{in} - \rho_{out} * \theta_{out} * u_{out} * A_{out} = \rho * u * A_{cross} * \Delta\theta \tag{9}$$

$\Delta\theta$ is $\theta_{in} - \theta_{out} = 2K$, and A_{cross} is the cross section area of the inflowing region, whereas u is the inflowing speed. $A_{cross} * u$ equals U, the volume transport given in Sverdrup ($7.1 * 10^6 \frac{m^3}{s}$). Which of equations 6 or 9 is the dominating term?
The size on equation 6 is determined by the volume that has heated, since the change in temperature with time is small. To assume that the whole of the Arctic Ocean has heated with 1 °C per 20 years is not correct, since the main part of the Atlantic Water is found in the Eurasian and Canadian Basins which has warmed at remarkable smaller rates. Let us assume that the heated volume is approximately the area of the inflow region (450km (the width of the inflow region) times 500m (the depth of the Atlantic Layer)) times a length, let us assume that this length is 2500km, that is the approximate distance from Spitsbergen to the Laptev Sea. This means that the heated volume V = $5.625 * 10^{14} m^3$. This gives us:

$$\frac{\rho\delta\theta * V}{t} \sim \frac{1 * 1028 * 5.625 * 10^{14}}{20 * 365 * 24 * 60 * 60} \sim 9 * 10^8 \tag{10}$$

$$\rho * u * A * \Delta\theta = \rho * U * \Delta\theta \sim 1028 * 7.1 * 10^6 * 2 \sim 1.5 * 10^{10} \tag{11}$$

The time derivative is more than 16 times smaller than the advection part of the equation, meaning that we can assume steady state. However, if we assume that the heated volume equals the total volume of the Atlantic Layer in the Arctic Ocean, that is the area ($9.5 * 10^{12} m^2$) times the depth of the Atlantic Layer (500 m), we get that the advection term is less than twice the size of the time derivative, and steady state is not a good simplification. Nevertheless, for this simple scaling we will assume steady state. The advection term is the dominant term on the left hand side of equation 5, so that the equation of concervation of heat is simplified to equation 12:

$$\nabla \cdot \rho\theta \overrightarrow{u} = S * \delta A \tag{12}$$

By applying Gauss theorem on the equation we get:

$$\oint\oint \rho\theta \overrightarrow{u} \cdot \overrightarrow{n} \delta A = \oint\oint S * \delta A$$
$$\leftrightarrow \rho * U * \Delta\theta = S * A_{tot} \tag{13}$$

,where S = $\frac{Q}{C_p}$, and A_{tot} is the total Arctic area. The heat transport, Q, is:

$$Q \approx \frac{U * \rho * \Delta\theta * C_p}{A_{tot}} \approx$$
$$\frac{7.1 * 10^6 \frac{m^3}{s} * 1028 \frac{kg}{m^3} * 2K * 4000 \frac{J}{kgK}}{9.5 * 10^{12} m^2} \approx$$
$$6 \frac{W}{m^2} \tag{14}$$

We assume that half of the total heat flux is transported upwards, and the other half is transported downwards into the interior. This means that the Atlantic Water in steady state has an upward heat flux of approximately $\underline{3}\frac{W}{m^2}$.
What would the estimated heat be if we did *not* assume steady state, but assumed that the total Arctic Atlantic volume heated at the same rate?

$$Q \approx \frac{\rho * C_P}{A_{tot}}(\frac{\delta\theta * V}{t} + U * \Delta\theta) \approx$$
$$\frac{1028\frac{kg}{m^3} * 4000\frac{J}{kgK}}{9.5 * 10^{12}m^2}(\frac{1K * 4.75 * 10^{15}m^3}{20 * 365 * 24 * 60 * 60s} + 7.1 * 10^6\frac{m^3}{s} * 2K) \approx$$
$$9\frac{W}{m^2} \qquad (15)$$

If we assume that half of the total heat flux is transported upwards, we get that the Atlantic Water, when it is *not* in steady state, has an upward heat flux of $\underline{4.5}\frac{W}{m^2}$.

These results suggest that there is enough heat within the Atlantic Layer to significantly influence the sea ice cover, since the amount of heat needed to melt 1 meter of ice in 20 years is approximately 6 times smaller than the heat flux from the Atlantic Layer in steady state, and 9 times smaller than the heat flux when the system is changing in time.
Earlier estimates of the Atlantic inflow from the west Spitsbergen Current are not as large as 7.1 Sv. Nevertheless, if we use a volume transport of 4 Sv, the heat flux in the Atlantic Layer in steady state is still 4 times larger than the amount of heat needed to melt 1 meter ice in 20 years, and 7 times larger when the system is changing in time, meaning that there are enough heat within the Atlantic Layer to significantly influence the sea ice cover, even at smaller volume transport rates.
More recent estimates by Schauer and Beszczynska-Möller (2009) result in even larger estimated heat fluxes from the Atlantic Layer. Let us assume that the inflowing and outflowing Atlantic Water is carried through the Fram Strait *and* through the Barents Sea branch. We use the estimated volume transports and temperatures from Schauer and Beszczynska-Möller (2009), see figure 31. The volume transports are now 11.5 Sv.
The area A is now the sum of the total Arctic area *and* the area of the Barents Sea (that is $1.3 * 10^{12}m^2$ (Mauritzen, 1996)), since these are the areas where the cooling occurs. We use the same approach as before, starting out with equation 5, however the equations will look a bit different, since the volume transports and temperatures are now different in the two regions. The heat flux, Q, in steady state (which is a good estimate in this case, since the time derivative is approximately 10 times less than the advection part of the equation when we assume that the whole of the Atlantic Layer has warmed at the same speed) is:

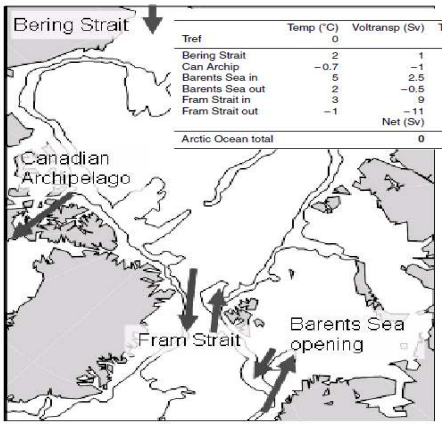

Tref	Temp (°C) 0	Voltransp (Sv)	Temp transport (TW)	Temp (°C) −273	Temp transport (TW)
Bering Strait	2	1	8	275	1100
Can Archip	−0.7	−1	2.8	272.3	−1089.2
Barents Sea in	5	2.5	50	278	2780
Barents Sea out	2	−0.5	−4	275	−550
Fram Strait in	3	9	108	276	9936
Fram Strait out	−1	−11	44	272	−11 968
		Net (Sv)	Heat transport (TW)		Heat transport (TW)
Arctic Ocean total		0	208.8		208.8

Figure 31: The estimated volume fluxes and temperatures flowing in and out of the Arctic Ocean. Figure and table from Schauer and Beszczynska-Möller (2009).

$$Q \approx \frac{\rho * C_p[(U_{fram-in} * \theta_{fram-in} + U_{bar-in} * \theta_{bar-in})]}{A_{arctic} + A_{barentssea}} - ... \\ \frac{\rho * C_p[(U_{fram-out} * \theta_{fram-out} + U_{bar-out} * \theta_{bar-out})]}{A_{arctic} + A_{barentssea}} \approx \\ \frac{1028\frac{kg}{m^3} * 4000\frac{J}{kgK}[(9 * 10^6\frac{m^3}{s} * 276K + 2.5 * 10^6\frac{m^3}{s}6 * 278K)]}{9.5 * 10^{12}m^2 + 1.3 * 10^{12}m^2} - ... \\ \frac{1028\frac{kg}{m^3} * 4000\frac{J}{kgK}[(11 * 10^6\frac{m^3}{s} * 272K + 0.5 * 10^6\frac{m^3}{s} * 275K)]}{9.5 * 10^{12}m^2 + 1.3 * 10^{12}m^2} \approx 19\frac{W}{m^2} \quad (16)$$

We still assume that half of the heat is transported upwards, meaning that we get an upward heat flux of $\underline{9.5}\frac{W}{m^2}$. This amount of heat could melt 1 meter of sea ice in one year, if all the heat was used for this purpose only. Nevertheless, we must remember that the cold halocline layer protects the surface from the underlying warm Atlantic Water, so that the main amount of the Atlantic heat will not reach the sea ice. However the influence of the Atlantic Water to the above-lying waters is getting more and more important as the upper interface between the Halocline Water and Atlantic Water continues to ascend into the 21^{st} century, and as the system moves away from steady state. I therefore argue that the ascent of the Atlantic Layer, which started in the 1990s is a key climate indicator which is important to continue monitor.

5.2 Pacific Layer influence

The Pacific Layer contains not by far the same amount of heat as the Atlantic Layer. From figure 22 it is clear that the Atlantic Water contains more than 10 times the heat in the Pacific Layer, that is $7 * 10^8\frac{J}{m^2}$ in the Pacific Layer com-

pared to $1 * 10^{10} \frac{J}{m^2}$ in the Atlantic Layer. In the Canadian Basin double diffusive staircases have been observed by ITP observations, with a vertical dimension of approximately 1 meter, but with horizontal dimensions of hundreds of kilometers (Timmermans et al., 2008). The estimated vertical heat fluxes are estimated as just $\frac{1}{10}$ of the average surface mixed layer heat flux to the sea ice, meaning that the vertical transport of heat from the Atlantic Layer in the Canadian Basin is unlikely to have significant influence on the heat budget in the upper ocean, and therefore unlikely to influence the sea ice melting. Timmermans et al. (2008) found that although we get more wind forcing due to less ice, the mixing rate required to get the Atlantic Water heat to contribute to the surface ocean heat budget in the Canadian Basin is maybe energetically impossible. However the Pacific Layer lies at shallow depths, with no halocline protecting the surface from the Pacific heat. The observed sea ice extent in the 21^{st} century was especially low in the area north of the Siberian and Alaskan coasts, that is in the Western Arctic Ocean. It cannot be a coincidence that the areas with the largest negative ice concentration anomalies in the 21^{st} century correspond to the area where warm Pacific Summer Water is observed just beneath the surface mixed layer, as proposed by Shimada et al. (2006). Observations show that the Pacific Water in the Beaufort Gyre is warmer and fresher in the 21^{st} century, making the water less dense, causing it to rise closer to the surface. I wanted to further investigate the positive anomaly in the Pacific Layer in 2007 in the Beaufort Gyre area (chapter 4.4), since this coincides both in time and location with the sea ice extent minimum seen in September 2007.
The summer of 2007 had unusual atmospheric pressure patterns over the Arctic which favoured warm air from the south over the coastal seas of eastern Siberia, leading to melting and also the ice being pushed from the coast into the Arctic Ocean (NSIDC, 2007). There were also fairly clear skies which favours ice melting during summer. This led to a positive anomaly in the surface air temperature reaching $+7\,^{\circ}$C over the Arctic Ocean, that is record high values (Richter-Menge et al., 2008). These high surface temperatures could alone be the cause of the anomalously low sea ice extent, and they could also increase the heat uptake in the ocean, and be the cause of the warm ocean temperature anomaly seen in 2007. Another alternative is that increased ocean temperatures in the Pacific Layer are independent of the increased surface air temperatures, contributing to an extra heat flux in the upper layer which enhanced the sea ice melting. To find out whether or not the last alternative could be true, daily mean Hovmoller ocean temperature diagrams for the Beaufort Gyre area were made from 2005-2009.
These results indicate that the daily mean Pacific Layer temperatures increased from October 2005 till January 2007 with up to $1.2\,^{\circ}$C, reaching temperatures close to $0\,^{\circ}$C in 2007, see figure 33. The warm period in the Pacific Layer started in December 2006 and lasted throughout October 2007. This means that the increased surface air temperatures are not the cause of the Pacific temperature increase. The warming in the Pacific Layer started out when there was sea ice present and exchange of heat from the atmosphere to the ocean is not efficient. However warm surface waters are evident in the late summer months due to increased heat uptake in the ocean because of ice free conditions. This warm surface water sinks down into the interior and contributes to the warm water at approximately 50-100 meters depth. The core of Pacific Water lies approximately 10 meters more shallow in 2007 compared to other years. In 2008 the

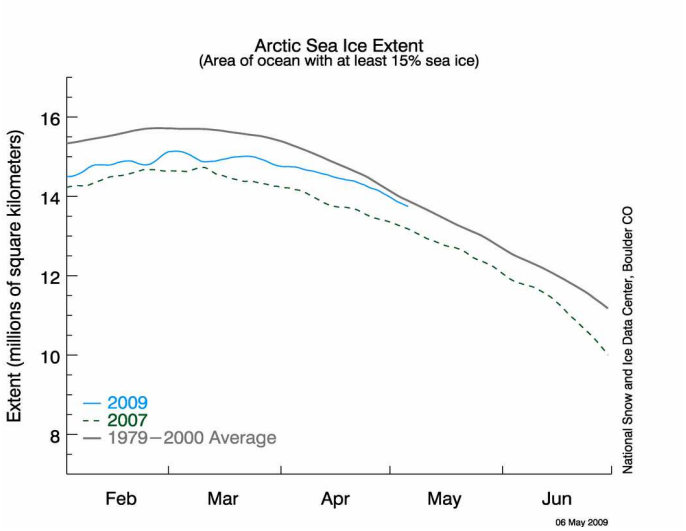

Figure 32: Daily Arctic Sea Ice extent in 2009 (blue line), 2007 (green dotted line) and from 1979-2000 (gray line) from the National Snow and Ice Data Center (NSIDC, 2009) .

temperatures are back to the values of 2006, and in 2009 the temperatures are back at the level seen in 2005, that is approximately $-1.2\,^{\circ}$C. The changes in the Atlantic Layer are small in the same time period, they are warmer with approximately $0.1\,^{\circ}$C throughout 2007. In 2009 there are colder Atlantic temperatures than the previous years with a decrease of approximately 0.2-0.3 $^{\circ}$C. Note that the spatial distribution and number of observations each year are different. In 2009 there are only 215 points located in a small cluster, whereas the number of observations in 2006 is 3266 and the spatial distribution is larger. We may be biased in 2009, nevertheless if we compare the sea ice extent with the extent of the extra warm water in the Pacific Layer the events are closely related! In 2009 there is so far no such event of warm Pacific Water evident, and the outlook for the sea ice so far is not really hinting at an extreme year, see figure 32 from the National Snow and Ice Data Center (NSIDC, 2009). Therefore I do not expect 2009 to be an extreme year for sea ice loss, nevertheless I cannot confirm this until September.

5.3 Future predictions

The observed hydrographic changes at the end of the 20^{th} and in the beginning of the 21^{st} century were not well represented in the HADLEY model. Nevertheless I wanted to see how the future predictions in both models were, since the negative trend in the sea ice cover in the 21^{st} century is fairly reproduced by both models.
Future predictions in the **HADLEY** model in the Arctic Ocean show large changes in the Atlantic water masses at the end of this century (results averaged over the whole Arctic Ocean), as shown in figure 34. The temperature in the At-

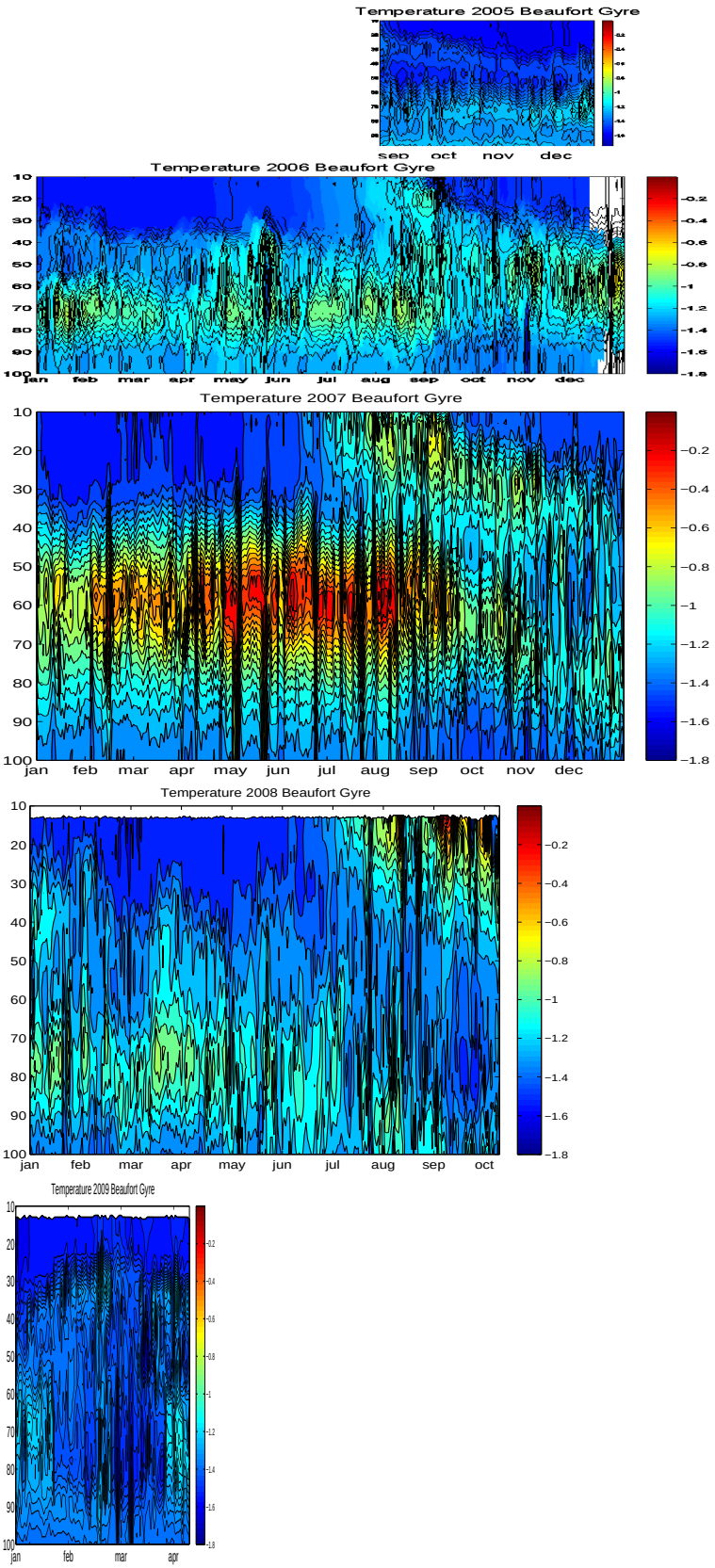

Figure 33: The daily mean ocean temperature in the Pacific Layer in the Beaufort Gyre area from 2005 (September) - 2009 (April).

lantic Layer is increased and the interface is lifted after the 2050s, and at the end of this century the temperatures in the Atlantic Layer reach 4 °C (compared to approximately 2.5 °C in the beginning of the 21^{st} century). The cold halocline layer lying above the warm Atlantic Water is thinning in the model. The summer (September) sea ice concentration is nearly 0% in the end of the 21^{st} century in the HADELY model, whereas the winter (January) ice concentration is larger than 70%, see figure 34.

The **NCAR** model had the most realistic results when compared to observations. The large observed changes in ocean temperature and sea ice concentration in the 21^{st} century are fairly represented. From figure 34 it is clear that the largest decrease in sea ice cover and the ascending Atlantic Water coincides in time. Even larger changes are projected in the 21^{st} century, after 2050 the Atlantic Water core temperature reaches 5.7 °C (compared to approximately 2 °C at the beginning of the 21^{st} century). The Atlantic Layer is lifted, and the overlying cold halocline layer is completely gone by the end of the century. The summer sea ice concentration is 0% at the end of this century, the winter sea ice concentration is less than 20%, as shown in figure 34. This indicates that the warming and lifting of the Atlantic Layer are highly correlated with the sea ice decline in the models.

To summarize: The NCAR model reproduces the changes seen after 1990 fairly well, both the warming and lifting of the Atlantic Layer and the decrease in sea ice concentration are fairly reproduced. The model predicts large changes in the ocean potential temperature after the 2050s. The cold halocline layer lying above the warm Atlantic Layer is completely gone in the NCAR model by the end of the century, and the summer sea ice concentration is as low as 0%, whereas the winter sea ice concentration is less than 20%. The changes in temperature in the HADLEY model at the end of the 20^{th} and in the beginning of the 21^{st} century are too small, nevertheless larger changes are predicted after the 2050s. The loss of sea ice in both models is closely related to ascent and warming of the Atlantic water masses, though in the HADLEY model this process does not kick in until post the year 2000. The ascent of the Atlantic Layer, which started in the 1990s is a key climate indicator. Presently the warm Atlantic Water cannot affect the Arctic sea ice significantly because the warm water is covered by a thick layer of cold halocline waters. However the analyse shows that the protective layer is thinning, and is projected to vanish within the 21^{st} century. Therefore I argue that the importance of the Atlantic Layer on the sea ice will be more important in the future.

5.4 The importance of anthropogenic emissions

From figure 30 from Wang and Overland (2009) it is clear that there is a close relationship between anthropogenic emissions of CO_2 and sea ice loss. The control runs show that anthropogenic forcing is necessary for the model to predict the large sea ice loss at the end of this century. The observed sea ice concentration is in good accordance with the NCAR A2 scenario in the beginning of the 21^{st} century, whereas the strong sea ice reduction in the 21^{st} century is not evident in a scenario with no further increase in CO_2 (committed scenario, the anthropogenic emissions are held fixed at the level in year 2000). Figure 35(a) shows the summer (September, blue), winter (January, red) and all year (black)

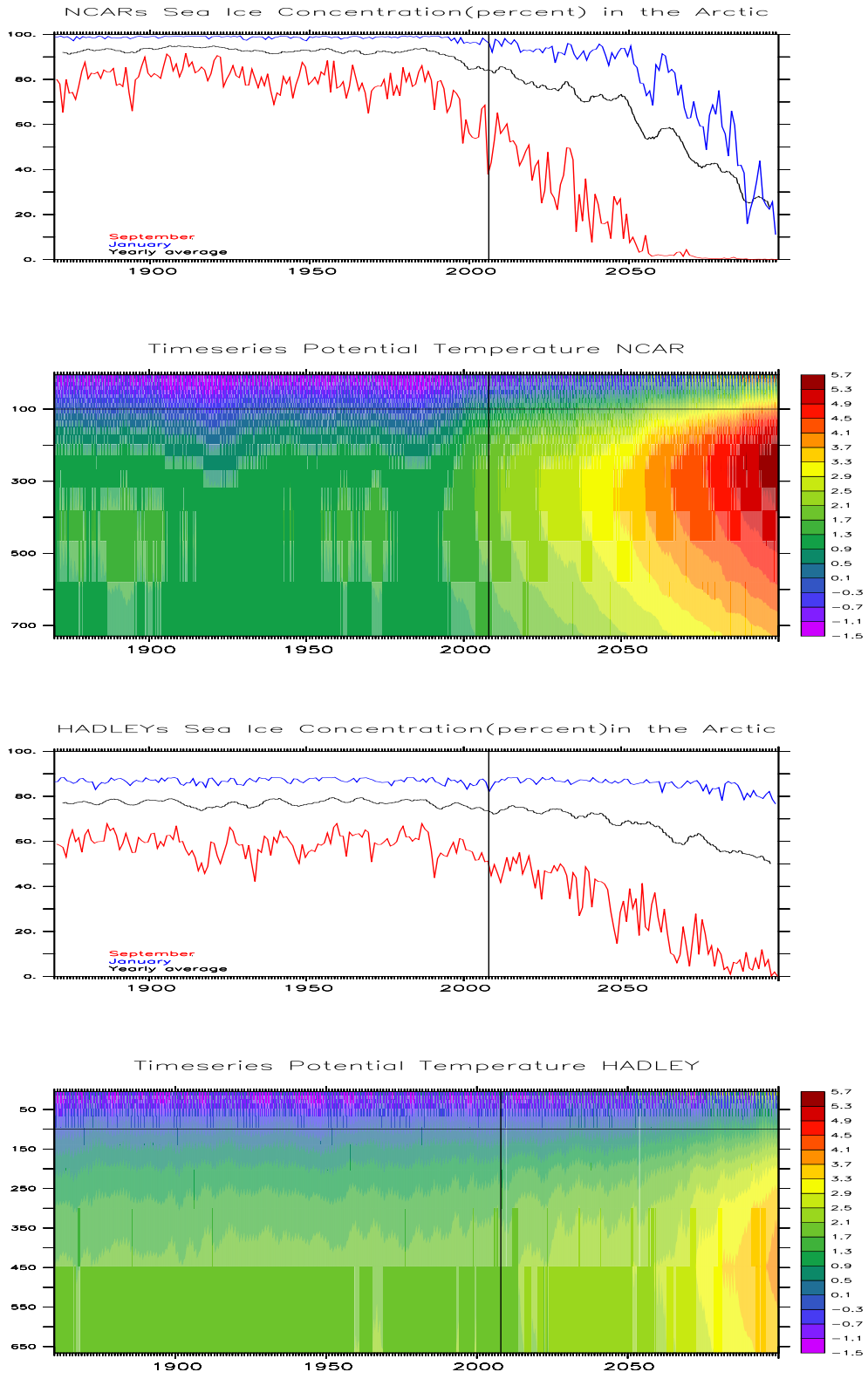

Figure 34: The sea ice concentrations (%) and potential temperature for the HADLEY (1860-2099) and NCAR (1870-2099) models. The sea ice concentrations are for September (blue), January (red) and yearly averaged (black), whereas the potential temperature are monthly data. Vertical black line indicates year 2009, horizontal black line indicates 100 meters.

sea ice concentration for a control run of the NCAR model with no further CO_2 increase. Compared to the sea ice concentrations with the high emission NCAR A2 scenario in figure 34 it is clear that anthropogenic forcing is necessary for the model to predict the large decrease in sea ice concentration at the end of this century.

Figure 35(b) shows that also there is a close relationship between anthropo-

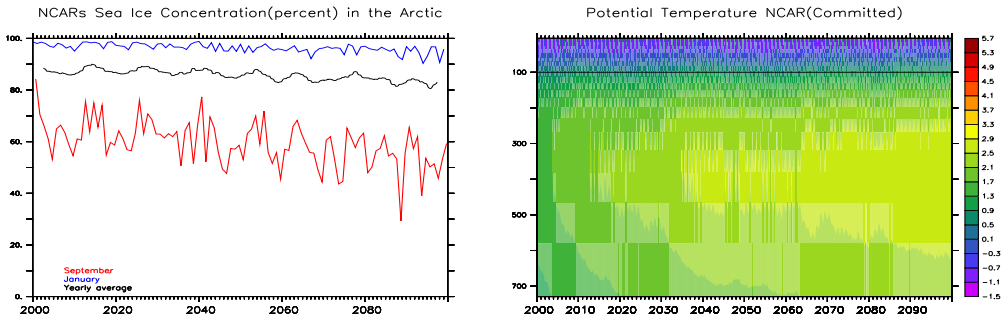

(a) (b)

Figure 35: (a): NCAR's sea ice concentration development in the 21^{st} century for September (blue), January (red) and yearly averaged (black) with no CO_2 increase (Committed scenario). (b): NCAR's potential temperature development in the 21^{st} century with no further CO_2 increase (Committed scenario).

genic emissions and the warming of the Arctic Ocean in the NCAR model. The strong increase in the ocean potential temperature after the 2050s that was evident in the A2 experiment runs (figure 34) is not seen in the committed scenario runs. Nevertheless a small temperature increase is seen, from approximately 2 °C in the beginning of the 21^{st} century to 2.5 °C at the end of this century. This implies that in the models anthropogenic emissions are responsible for the largest part of the temperature increase in the Arctic Ocean in the 21^{st} century. Without further anthropogenic forcing there are no extensive warming and lifting of the Atlantic Layer, neither a dramatic sea ice retreat. The anthropogenic emissions of green house gasses can be controlled, whereas how to stop the large changes in the Arctic Ocean is a big question. Because of the large heat capacity of the ocean, there is a significant time lag in the oceans' response to atmospheric changes. It will take time, if it is even possible, to reverse the large oceanic changes.

To summarize, neither change occur in model runs without continued atmospheric forcing. The large changes that were evident in the A2 experiment runs are not seen in the committed scenario. This implies that in the models increased anthropogenic emissions are necessary for the ascent and warming of the Atlantic Layer, and also the sea ice concentration decline. As mention in chapter 4.5 the observed CO_2 concentration is so far larger than any of the IPCC

CO_2 emission scenarios (as shown in figure 27 from Raupach et al. (2007)). If this develops further it could mean that the IPCC scenarios are too conservative, and that we are facing even more dramatic changes than projected by the NCAR and HADLEY models.

6 Conclusions

Large changes in the hydrographic properties (potential temperature, salinity and density) are observed in the Atlantic and Pacific layers in the Arctic Ocean, the large changes started in the 1990s and continued to increase in the 21^{st} century. The changes are summarized in figure 36.
This chapter tries to answer the seven questions asked in the introduction.

Changes compared to the 1980s	**SVAL:** North of Spitsbergen Region	**SIB:** Siberian Continental Shelf Area	**EUR:** Central Eurasian Basin	**CAN:** Central Canadian Basin
Error estimates:	±0.8 ºC and ±0.2 units in the Atlantic layer.	±0.5 ºC and ±0.2 units in the Atlantic layer.	±0.4 ºC and ±0.1 units in the Atlantic layer.	±0.4 ºC and ±0.1 units in the Atlantic water. ±0.425 ºC and 0.125 units in the Pacific layer.
Hyrdrographic changes in the Atlantic Layer	Up to 3.5ºC ±0.8 ºC higher temperatures. Salinities 0.4 ±0.2 units higher.	0.4-1.5ºC ±0.5 ºC higher temperatures. Salinities 0.3 ±0.2 units higher.	0.2-0.5ºC ±0.4 ºC higher temperatures. Salinities 0.2 ±0.1 units higher.	Up to 0.5ºC ±0.4 ºC higher temperatures. Salinities 0.2 ±0.1 units higher.
Hydrographic changes in the Pacific Layer	No Pacific influence	No Pacific influence	Some Pacific influence on the Canadian side of Lomonosov, but not significant changes.	0.1- 0.6ºC ±0.425 ºC higher temperatures. Salinities up to 1 ±0.125 units *fresher*.
Change in depth of the upper interface of Arctic Atlantic Water	Large year to year variability, record low interface in the 21st century	40-60 ± 10 m. higher interface in the 21st century.	The interface ascended with up to 50 ± 10 m. in the 1990s, no further ascend in the 21st century.	The interface ascended with 30 ± 10 m. in the 1990s, continued to ascend with 30 ± 10 more meters in the 21st century.

Figure 36: Table summary of the hydrographic changes seen in the 21^{st} century compared to the historical data.

How much warmer has the Arctic Ocean become since the 1950s?
The warming started in the 1990s and continued to increase in the 21^{st} century. The warming in the Atlantic Layer is largest in the inflow region north of Spitsbergen. The Atlantic temperature in this region is $3.5\pm0.8\,^{\circ}$C higher in the 21^{st} century compared to the historical data. Along the Siberian Continental Shelf Area the Atlantic temperature increase is $0.4\text{-}1.5\pm0.5\,^{\circ}$C, whereas in the Eurasian and Canadian Basins the warming in the 21^{st} century is up to $0.5\pm0.4\,^{\circ}$C. The Pacific Layer in the Canadian Basin is $0.1\text{-}0.6\pm0.425\,^{\circ}$C warmer in the 21^{st} century compared to the historical data.
What are the main hydrographic changes that have taken place?

The main hydrographic changes that have taken place are increased temperatures accompanied by salinification in the Atlantic Layer, and freshening in the Pacific Layer. The salinity north of Spitsbergen is 0.4 ± 0.2 units higher in the 21^{st} century compared to the historical data. The salinity in the other regions of the Arctic Ocean is higher with 0.3 ± 0.2 units along the Siberian Coast, and 0.2 ± 0.1 units in the Canadian and Eurasian Basins. There are less dense waters in the core of the Atlantic Layer, however from the start of the Atlantic Layer and down to the core the density is often higher than the EWG data due to increased salinities in the 21^{st} century.
The warming in the Pacific Layer is accompanied by a freshening of up to 1 ± 0.125 unit in the 21^{st} century. This makes the Pacific Layer less dense in the 21^{st} century.
Also the interface between the cold Halocline Water and the underlying warm Atlantic Water has been lifted in the 21^{st} century, with up to 60 meters. In the NCAR and HADLEY models the warming and lifting of the Atlantic Layer were highly correlated with the sea ice reduction. This implies that the Atlantic Water will be more important to the sea ice in the future as the halocline layer is thinning.

Are there some parts of the Arctic that has not really changed a lot?

The observed changes in the Atlantic Layer in the Eurasian and Canadian Basins are not by far as large as the changes closer to the Fram Strait. In the Eurasian Basin the changes were often larger in the 1990s, with decreasing values going into the 21^{st} century. However the temperatures and salinities in the Eurasian and Canadian Basins in the 21^{st} century are still larger than the historical data, with positive temperature anomalies (with the EWG data set as reference values) almost all years from 1991-2008. The increased inflowing temperatures in the Atlantic Layer imply that the heat transported to the surrounding ocean must have increased in the 21^{st} century, since the rate of warming is less in the Eurasian and Canadian Basins. However there is a significant time lag between the regions, and this could partly explain the differences.

Do the changes seen come from pulses or trends?

There are events of warm pulses in the Arctic Ocean in the Atlantic Layer, and also in the Pacific Layer in the Canadian Basin. The anomalies propagate along the Arctic circulation. The changes seen at the end of the 20^{th} and in the beginning of the 21^{st} century exceed earlier widespread Atlantic Layer changes. At depths corresponding to the Atlantic and Pacific Layer there are positive anomalies in almost all years from the 1990s till present, and the anomalies are mainly larger in the 21^{st} century than in previous years. Thus the pulses in recent years are superimposed on a long term warming trend rather than being the main signal.

How well do the IPCC models reproduce the changes seen at the end of the 20^{th} and in the beginning of the 21^{st} century, and what are Arctic's future prospect?

The **NCAR** model reproduces the observed changes in the Arctic Ocean seen in recent decades fairly well: Both the ascending interface depths and increasing temperatures in recent decades are well simulated. However the Arctic circulation is not well represented by the model. NCAR has the most realistic sea ice extent when compared to observations, and the negative trend in sea ice concentration is well reproduced. However the spatial distribution of sea ice in the model is not correct.

Also the **HADLEY** model reproduces the negative trend in sea ice concentration, but the concentrations are overestimated. The model does not simulate the observed temperature increase in the Arctic Ocean seen in recent decades, neither the lifted Atlantic interface.
In the HADLEY model the temperature in the Atlantic Layer is increased and the interface is lifted after the 2050s, and at the end of this century the temperatures in the Atlantic Layer reach 4 °C (compared to approximately 2.5 °C in the beginning of the 21^{st} century). The cold halocline layer lying above the Atlantic Layer is thinning. The summer (September) sea ice concentration is nearly 0% by the end of the 21^{st} century, whereas the January ice concentration is larger than 70%.
Even larger changes are projected in the 21^{st} century with the NCAR model, both in temperature, lifting of the Atlantic Layer and in sea ice concentrations. After the 2050s the Atlantic Water core temperature reaches 5.7 °C (compared to approximately 2 °C in the beginning of the 21^{st} century). The cold halocline layer is completely gone by the end of this century. The summer sea ice cover in the NCAR model is 0% at the end of this century, the January sea ice concentration is less than 20%.
Can these models shed any light on the significance of the changes we have seen in the Arctic hydrography?
In both of the NCAR and HADLEY models the loss of sea ice is closely related to ascent and warming of the Atlantic water masses. In the future the loss of sea ice is largest in the NCAR model, and so far this is the model that best represents the observed changes. The abrupt sea ice melting at the end of the 1990s is correlated in time with the Atlantic Layer lifting and warming.
From the models it is clear that the halocline barrier lying above the warm Atlantic Layer will disappear at the end of the 21^{st} century. Without this cold lid the sea ice will be much more exposed to the warm Atlantic Layer. The results from chapter 5.1 suggest there is enough heat within the Atlantic Layer to significantly influence the sea ice cover, since the amount of heat needed to melt 1 meter of ice in 20 years is 6 times smaller than the heat flux from the Atlantic Layer in steady state, and 9 times smaller than the heat flux when the system is changing in time. The influence of the Atlantic Water to the above-lying waters is getting more and more important as the upper interface between the Halocline Water and Atlantic Water continues to ascend into the 21^{st} century, and as the system moves away from steady state. The large changes do not happen in the models without further anthropogenic forcing.
Are there any connections between the observed changes in the ocean and the sea ice?
The observations imply that the sea ice cover in the Canadian Basin is closely linked to events of warm Pacific Water. The waters were especially warm in 2007, when a warm pulse that lasted for almost a year coincided in time and location with the sea ice extent minimum in 2007. In 2009 there is so far no such event of warm Pacific Water evident, and the outlook for the sea ice so far is not really hinting at an extreme year. Whether the events of warm water in this region will occur more frequently in the future needs more investigation.
Because of the different rate of Atlantic warming in the inflow region and the Eurasian and Canadian Basins, heat transport from the Atlantic Layer could be higher than in previous decades (it could also partly be explained by slowness in the system). There is enough heat within the Atlantic Layer to significantly

influence the sea ice cover, however the surface is protected from the heat by the cold halocline. Nevertheless, the increased heat loss from the Atlantic Water in the Arctic must sooner or later contribute to change the energy balance up towards the sea ice, as the Atlantic Layer warms and ascends and the cold protective halocline layer is thinning. I therefore argue that the ascent of the Atlantic Layer, which started in the 1990s is a key climate indicator which is important to continue monitor. If the different speed of warming in the inflow regions compared to the Central Eurasian and Canadian Basins is associated with time lag, or if a larger amount of heat than in previous decades is lost to the surrounding ocean needs further investigation.

I suggest that the Arctic Ocean is going towards a warmer state, and that the system is moving away from steady state. The Arctic is a vulnerable region, and if this is a development which cannot be reversed we are facing large challenges in our immediate future.

References

Arctic Climatology Project (2000). Environmental Working Group joint U.S.-Russian sea ice atlas. Ann Arbor, MI: Environmental Research Institute of Michigan in association with the National Snow and Ice Data Center. CD-ROM.

Bindoff, N., J. Willebrand, A. V. Artale, Cazenave, J. Gregory, S. Gulev, K. Hanawa, C. L. Quéré, S. Levitus, Y. Nojiri, C. Shum, L.D.Talley, and A. Unnikrishnan (2007). Contribution of Working Group I to the Fourth Assessment Report of the Intergovernmental Panel on Climate Change (IPCC): Observations: Oceanic Climate Change and Sea Level. *Climate Change 2007: The Physical Science Basis*.

Boyd, T. J., M. Steel, R. D. Muench, and J. T. Gunn (2002). Partial recovery of the Arctic Ocean halocline. *Geophys. Res. Lett. 29*(14, doi:10.1029/20001GL014047).

CCCma (2005). The Canadian centre for climate modelling and analysis. Digital media: http://www.cccma.ec.gc.ca/data/cgcm3/cgcm3_forcing.shtml.

Coachman, L. K. and C. A. Barnes (1963). The movement of Atlantic Water in the Arctic Ocean. *Arctic 16*(1), 8–16.

Cokelet, E. D., N. Tervalon, and J. G. Bellingham (2008). Hydrography of the West Spitsbergen Current, Svalbard Branch: Autumn 2001. *J. Geophys. Res. 113*(C01006, doi:10.1029/2007JC004150).

Cook, J. (2006). The circulation system in the Arctic Ocean. Digital media: http://www.whoi.edu/page.do?pid=10897&i=61&x=19, illustration by Jack Cook, Woods Hole Oceanographic Institution.

Dmitrenko, I., I. Polyakov, S. A. Kirillov, L. A. Timokhov, I. E. Frolov, V. T. Sokolov, H. L. Simmons, V. V. Ivanov, and D. Walsh (2008). Toward a warmer Arctic Ocean: Spreading of the early 21st century Atlantic Water warm anomaly along the Eurasian Basin margins. *J. Geophys. Res. 113*(C05023, doi: 10.1029/2007JC004158).

Fetterer, F. and K. Knowles (2008). Sea ice index. Digital media: ftp://sidads.colorado.edu/DATASETS/NOAA/G02135/Sep/N_09_plot.png.

Fosså, J. H. (2009, 31. March). Interview TV2. Marine biologist at the institute of Marine Research in Bergen Norway, also available at web: http://www.tv2nyhetene.no/article2653824.ece.

Graversen, R., T. Mauritsen, M. Tjernström, E. Källén, and G. Svensson (2008). Vertical structure of recent Arctic warming. *Nature 541*, 53–56, doi:10.1038/nature06502.

Grotefendt, K., K. Logemann, D. Quadfasel, and S. Ronski (1998). Is the Arctic Ocean warming? *J. Geophys. Res. 103*(c12), 27 679–27 687.

Hassol, S. J. (2004). *ACIA, Impacts of a Warming Arctic: Arctic Climate Impact Assessment*, Chapter Keyfinding 2: Arctic warming and its consequences have worldwide implications, pp. 34–39. Cambridge University Press,http://www.acia.uaf.edu.

Karcher, M. J., R. Gerdes, F. Kauker, and C. Köberle (2003). Arctic Warming: Evolution and spreading of the 1990s warm event in the Nordic seas and in the Arctic Ocean. *J. Geophys. Res. 108*(C2, doi:10.1029/2001JC001265).

Knauss, J. A. (2005). *Introduction to physical oceanography*, pp. 260–262. University of Rhode Island.

Lemke, P., J. Ren, R. Alley, I. Allison, J. Carrasco, G. Flato, Y. Fujii, G. Kaser, P. Mote, R. Thomas, and T. Zhang (2007). Contribution of Working Group I to the Fourth Assessment Report of the Intergovernmental Panel on Climate Change (IPCC): Observations: Changes in Snow, Ice and Frozen Ground. *Climate Change 2007: The Physical Science Basis*.

Mauritzen, C. (1996). Production of dense overflow waters feeding the North Atlantic across the Greenland-Scotland Ridge. Part2: An inverse model. *Deep-Sea Research 43*(6), 807–835.

Meehl, G., T. Stocker, W. Collins, P. Friedlingstein, A. Gaye, J. Gregory, A. Kitoh, R. Knutti, J. Murphy, A. Noda, S. Raper, I. Watterson, A. Weaver, and Z.-C. Zhao (2007). Contribution of Working Group I to the Fourth Assessment Report of the Intergovernmental Panel on Climate Change (IPCC): Global Climate Projections. *Climate Change 2007: The Physical Science Basis*.

Morgan, P. and L. Pender (2006). Sea Water Package tool for MATLAB. Digital media: http://www.cmar.csiro.au/datacentre/ext_docs/seawater.htm.

National Geophysical Data Center (2001). Bathymetric and topographic map over the Arctic. National Oceanic and Atmospheric Administration, U.S. Department of Commerce, digital media: http://www.ngdc.noaa.gov/mgg/image/IBCAO_betamap.jpg.

National Weather Service Climate Prediction Centre (2008). Monitoring Weather and Climate. Digital media: http://www.cpc.noaa.gov/products/precip/CWlink/pna/JFM_season_nao_index.shtml.

Nishino, S., K. Shimada, M. Itoh, M.Yamamoto-Kawai, and S. Chiba (2008). East-West differences in water mass, nutrient, and chlorophyll *a* distributions in the sea ice reduction region of the western Arctic Ocean. *J. Geophys. Res. 113*(C00A01, doi:10.1029/2007JC004666).

NSIDC (2007). National Snow and Ice Data Center: Arctic Sea Ice News from 2007. Digital media: http://www.nsidc.org/arcticseaicenews/2007.html#1October.

NSIDC (2008). Arctic sea ice news. Digital media: http://nsidc.org/news/press/20081002_seaice_pressrelease.html.

NSIDC (2008). National Snow and Ice Data Center: Sea ice index. Digital media: http://nsidc.org/news/press/2007_seaiceminimum/images/20070904_extent.png.

NSIDC (2009). National Snow and Ice Data Center: Sea Ice Trends In Extent. Digital media: http://www.nsidc.org/data/seaice_index/images/daily_images/N_timeseries.png.

Pawlowicz, R. (2005). M-map mapping tool for MATLAB. Digital media: http://www.eos.ubc.ca/∼rich/map.html.

Polyakov, I., G. Alekseev, L. Timokhov, U. Bhatt, R. Colony, H. L. Simmons, D. Walsh, J. Walsh, and V. Zakharov (2004). Variability of the Intermediate Atlantic Water of the Arctic Ocean over the last 100 years. *Journal of Climate 17*(23), 4485–4497.

Quadfasel, D., A. S. D. Wells, and A. Tunik (1991). Warming in the Arctic. *Nature 350*, 385, doi:10.1038/350385a0.

Raupach, M. R., G. Marland, P. Ciais, C. L. Quéré, J. G. Canadell, G. Klepper, and C. B. Field (2007). Global and regional drivers of accelerating CO2 emissions. *PNAS 104*, 10288–10293.

Richter-Menge, J., J. Overland, M. Svoboda, J. Box, M. Loonen, A. Proshutinsky, V. Romanovsky, D. Russell, C. Sawatzky, M. Simpkins, R. Armstrong, I. Ashik, L.-S. Bai, D. Bromwich, J. Cappelen, E. Carmack, J. Comiso, B. Ebbinge, I. Frolov, J. Gascard, M. Itoh, G. Jia, R. Krishfield, F. McLaughlin, W. Meier, N. Mikkelsen, J. Morison, T. Mote, S. Nghiem, D. Perovich, I. Polyakov, J. Reist, B. Rudels, U. Schauer, A. Shiklomanov, K. Shimada, V. Sokolov, M. Steele, M.-L. Timmermans, J. Toole, B. Veenhuis, D. Walker, J. Walsh, M. Wang, A. Weidick, and C. Zöckler (2008). Arctic Report Card 2008. *Digital media: http://www.arctic.noaa.gov/reportcard*.

Rothrock, D., Y. Yu, and G. Maykut (1999). Thinning of the Arctic sea-ice cover. *Geophys. Res. Lett. 26*(23), 3469–3472.

Schauer, U. (2008, November). Heat in the Arctic Ocean. Personal communication.

Schauer, U. and A. Beszczynska-Möller (2009). Problems with estimating oceanic heat transport - conceptual remarks for the case of Fram Strait in the Arctic Ocean. *Ocean Sci. Discuss 6*(2), 1007–1029.

Shimada, K., E. Carmack, K. Hatakeyama, and T. Takizawa (2001). Varieties of shallow temperature maximum waters in the Western Canadian Basin of the Arctic Ocean. *Geophys. Res. Lett. 28*(18), 3441–3444.

Shimada, K., T. Kamoshida, M. Itoh, S. Nishino, E. Carmack, F. McLaughlin, S. Zimmermann, and A. Proshutinsky (2006). Pacific Ocean inflow: Influence on a catastrophic reduction of sea ice cover in the Arctic Ocean. *Geophys. Res. Lett. 33*(L08605, doi:10.1029/2005GL025624).

Shimada, K., F. McLaughlin, E. Carmack, A. Proshutinsky, S. Nishino, and M. Itoh (2004). Penetration of the 1990s warm temperature anomaly in the Atlantic Water in the Canadian Basin. *Geophys. Res. Lett. 31*(L20301, doi:10.1029/2004GL020860).

Steele, M. and T. Boyd (1998). Retreat of the cold halocline layer in the Arctic Ocean. *J. Geophys. Res. 103*(C5), 10 419–10 435.

Steele, M., J. Morison, W. Ermold, I. Rigor, M. Ortmeyer, and K. Shimada (2004). Circulation of summer Pacific halocline water in the Arctic Ocean. *J. Geophys. Res. 109*(C02027, doi:10.1029/2003JC002009).

Swift, J., K. Aagard, L. Timokhov, and E. G. Nikiforov (2005). Long-term variability of Arctic Ocean waters: Evidence from a reanalysis of the EWG data set. *J. Geophys. Res. 110*(C03012, doi:10.1029/2004JC002312).

Talley, L. D., G. L. Pickard, W. J. Emery, and J. H. Swift (2009). *Descriptive Physical Oceanography: An Introduction* (6 ed.). Chapter 12: The Arctic and Northern Polar Oceans.

The Climatic Research Unit (CRU) (2008). The combined global land and marine surface temperature record from 1850-2008. Digital media: http://www.cru.uea.ac.uk/cru/info/warming/.

The CMIP3 archive (2004). The World Climate Research Program's (WCRP's) Coupled Model Intercomparison Project phase 3 (CMIP3) multi-model dataset.

Timmermans, M.-L., J. Toole, R. Krishfield, and P. Winsor (2008). Ice-Tethered Profiler observations of the double diffusive staircase in the Canadian Basin thermocline. *J. Geophys. Res. 113*(C00A02, doi:10.1029/2008JC004829).

Trenberth, K., P. Jones, P. Ambenje, R. Bojariu, D. Easterling, A. K. Tank, D. Parker, F. Rahimzadeh, J. Renwick, M. Rusticucci, B. Soden, and P. Zhai (2007). Contribution of Working Group I to the Fourth Assessment Report of the Intergovernmental Panel on Climate Change (IPCC): Observations: Surface and Atmospheric Climate Change. *Climate Change 2007: The Physical Science Basis*.

Visbeck, M. (2008). North Atlantic Oscillation. Digital media: http://www.ldeo.columbia.edu/NAO.

Walsh, J. E. (2007). *ACIA Scientific Report*, Chapter 6: Cryosphere and Hydrology, pp. 192–193. ACIA Secretariat and Cooperative Institute for Arctic Research University of Alaska Fairbanks.

Wang, M. and J. E. Overland (2009). A sea ice free summer Arctic within 30 years? *36*(L07502, doi:10.1029/2009GL037820). Geophys. Res. Lett.

Woodgate, R., T. Weingartner, T. Whitledge, R. Lindsay, and K. Crane (2008). THE PACIFIC GATEWAY TO THE ARCTIC: QUANTIFYING AND UNDERSTANDING BERING STRAIT OCEANIC FLUXES. Russian American Long-term Census of the Arctic. Digital media: http://www.arctic.noaa.gov/aro/russian-american/2008/*THE_PACIFIC_GATEWAY_TO_THE_ARCTIC*.pdf.

Woods Hole Oceanographic Institution (2007). ITP-data. Digital media: http://www.whoi.edu/page.do?pid=23096.

Woods Hole Oceanographic Institution (WHOI) (2007). ITP-data. Digital media: http://www.whoi.edu/itp.

List of Figures